„POLITEHNICA” UNIVERSITY OF BUCHAREST

FACULTY Applied chemistry and materials science
DEPARTMENT Chemical engineering department

Senate Decision No. 623 of 23.11.2020

DOCTORAL THESIS ABSTRACT

CONTROL OF ANAEROBIC PROCESSES FROM THE PRODUCTION OF BIOFUELS

(Keywords: ABE fermentation, statistical modeling, PVA-BC membrane, biofuels)

Author: Ing. Patrichi Claudia Ana Maria

Scientific Coordinator: Prof. dr. ing. Tănase Dobre

EVALUATION BOARD OF THE DOCTORAL THESIS

President	Prof. Dr. Ing. Dănuț-Ionel VĂIREANU	**from**	Politehnica University of Bucharest
PhD Supervisor	Prof. Dr. Ing. Tănase DOBRE	**from**	Politehnica University of Bucharest
Reviewer	Prof. Dr. Ing. Claudia MUNTEAN	**from**	Ovidius University of Constanta
Reviewer	Conf. Dr. Ing. Adina GAVRILĂ	**from**	Politehnica University of Bucharest
Reviewer	Prof. Dr. Ing. Alexandru OZUNU	**from**	Babeș-Bolyai University of Cluj Napoca

BUCUREȘTI
2020

CONTENTS

CHAPTER 1

Introduction

In this paper, the problem of controlling the production of fermentation biofuels by simpler or more complicated methods was addressed. This field of fermentation biofuels is of great interest in the world, with current development directions being geared to renewable energy sources and technologies, including the genetic development of new fermenting micro-organisms, which require low energy consumption but also long-term sustainability.

In a world increasingly concerned about saving resources, preserving existing ones and leaving behind an environment that is as little as possible altered by destructive human action, micro-organisms, once considered fearful enemies, can now be reliable allies. These can be a viable alternative in a multitude of bioprocesses ranging from the production of biosurfactants to waste water treatment to the synthesis of biosolvents.

The processes that take place at the gas-liquid interface are complex processes and generally difficult to study. When these processes also involve the action of microorganisms, the challenge and difficulty of research is amplified.

Bioethanol is the most important biofuel produced by fermentation of sugars from different biomass species. In this work a coupled process is proposed in one of the chapters to recover bioethanol obtained from the fermentation of sugars with yeast of the Saccharomyces cerevisiae class.

Due to the complexity of the topic addressed, two major directions have been selected, focusing both on literature and experimental research.

A first direction is to establish mathematical models for bioprocesses, which are customized to an anaerobic process and to the fermentation of EBA. The main goal was to achieve a higher degree of detail and understanding of an anaerobic bioprocess coupled with the in situ separation of reaction products. In order to achieve this, the theoretical part has been structured starting from the modeling of bioprocesses in general and the need to associate a mathematical model with a complex phenomenon, given the degree of complexity of these models. The determination of the complexity of the model shall take into account the purpose of implementing the model. The customization was carried out for an important anaerobic bioprocess in the production of biofuels, i.e. the biosynthesis EBA (acetone-butanol-ethanol), regarded as a semi-continuous process taking place in a mixing bio-reactor.

The challenge subsequently arose from the attempt to couple this bioprocess, in which inhibition due to reaction products, i.e. butanol, occurs, with a process of separation and recovery of solvents in situ. In order to remove butanol which, although desirable as a product, is also the main enemy of the microbial population, which is sensitive to the toxicity of this solvent, the process was coupled with the gas stripping separation of the three solvents.

The second research direction of both the literature and the experimental research was to obtain the rigid membranes of polyvinyl alcohol (PVA)-biocellulose (BC) on ceramic support and to determine the total flow rate of permeat, respectively their selectivity in the ethanol-water system. Particular importance shall also be given to establishing the mathematical model of the two-stage pervaporation process for the production of concentrated ethanol. The information being focused on the issue of modelling, simulation and even optimisation of this procedure, in particular when using the batch and fed-batch bioreactor.

In all three processes addressed in the paper the bioreactor is the equipment whose construction, operation and control depends on productivity.

Mixing bioreactors provide high transfer speeds for both mass and heat, as well as excellent mixing of the reaction environment. In these systems there are a large number of variables that influence the mass transfer and the mixing. Of these the most important are: the speed of the stirrer, the number of mixers and the gas flow rate used.

One phase of experimental research aims at studying the production of biogas and controlling its production in installations.

This paper provides descriptions, general and experimental data on the operation of a coupled process "biological wastewater purification - biogas generation from activated sludge" in a large plant, up to 500000 m^3/day grey water and rainwater, characteristic of a large city.

CHAPTER 2

Anaerobic fermentation biofuel. General. Technological analysis

Bioethanol, biobutanol and biogas are the three anaerobic fermentation fuels of great economic interest in the current energy context. This chapter insists on fixing the energy context and shows the place of these fuels within it.

2.6 Biofuels: biobutanol, bioethanol and biogas and control of anerobic processes

In opening this paragraph we return to the idea of the duality using of fossil fuels in energy production and to support transport of whatever kind it may be. Now in the world the first energy concern caused by the widespread use of fossil fuels, formed and stored underground for millions of years, is that the current vegetation on Earth cannot treat the carbon dioxide emitted through photosynthesis. The result is the greenhouse effect, with the consequent climate change . Climate change attributed to increased CO_2 emissions and other greenhouse gases obliges humanity to develop alternative energy sources. The resource at hand is biomass, either fresh or residual, which must be processed in such a way as to become effectively usable as an energy vector.

The second reason why man must move towards renewable energy resources is related to the demographic explosion that amplifies the concern, imposed by the requirements of the fourth industrial revolution, by the depletion of general oil reserves [30]. One example is that the world's ten largest economies (the United States, China, Germany, England, France, Italy, India, Brazil, Russia, Canada) with certain exceptions (the U.S., Russia, Brazil), as well as most other nations, depend on oil. The consequences of inadequate oil availability could thus be extremely severe. This is why it brings many incentives to explore alternative energy sources.

Of the four universally recognized biofuels, biodisel, bioethanol, biobutanol and biogas, the last three have in common that they result from the fermentation of organic substrates as a source of carbon. It may also be added that bioethanol and biobutanol have fermentable sugars as their substrate. Before pointing out what the three fermentation processes have in common and what elements their control refers to, in the following are brought to attention the data of primary characterization and engineering interest of each process.

2.6.1 General aspects regarding the production of biobutanol (fermentation butanol)

Microorganisms in EBA synthesis. In general, the bacterial systems of the class Clostridia, positive gram in stem form, with sporulation and multiplication under typical anaerobic conditions, contain classes with solvent-generating behavior (acetone, butanol, ethanol). Specifically, the leading representative of this class of microorganisms Clostridium acetobutylicum is a gram-positive bacillus easy to find in soil and other media, mesophilic with field of activity 10-60^{0}C and saccharahitic (can decompose sugar). Solvent-generating clostridia species can use a wide variety of substrates, from simple monosaccharides such as pentoses (fructose) and hexoses (glucose) to more or less complex polysaccharides [31]. How it is known the growth of bacteria (multiplication of bacteria) generally needs sources of nitrogen, so the yeast extract, rich in protein, is used for a good growth and production of solvents. The multiple recipes for culture media show that nutrient requirements for bacterial growth of clostridia are not complicated. A specific characteristic of the production of solvents (EBA) by clostridial bacterial systems, a characteristic also found in fermentation with biogas production (methanogenesis) and even in alcoholic fermentation, is that the fermentation process takes place, as shown in Figure 2.9, in two stages. The first stage is called the acidogenic stage, during which the enzyme systems of clostridian bacteria activate the pathway for the formation of acetate and butyrate acids so that hydrogen and carbon dioxide are majority products. In relation to the cell growth curve [36], the acidogenic stage usually occurs during the exponential growth (multiplication) phase of the bacterial system [37].

The second stage in fermentation is the stage called solventogen, during which acids are re-assimilated to be used in the production of acetone, butanol and ethanol (or isopropanol instead of acetone in some cases of the use of Clostridium Beijerinckii culture). The transition from the acidogenic to the solventogenic stage is the result of a dramatic change in the pattern of genetic expression, in the sense that at the cellular level in Clostridium Acetobutylicum appears the transcription of the production of solventogenic enzymes (enzymes nominated on the continuous lines characterizing the evolution of solventogenesis in the metabolic scheme given in Figure 2.9).

With reference to the 17 enzymatic chemical reactions noted in Figure 2.9 (here the name of the enzyme supporting a reaction is written in gray), which take place in the cells of the bacterium, it should be noted that they are supported from an energy point of view and reactive by the presence (e.g. : $Glucose + NAD \xrightarrow[ATP]{} Pyruvic\ acid + NADH$) and production (e.g. $Acetil\ triphosphate \xrightarrow[acetate\ kinase]{} Acetic\ acid + ATP$) of triphosphoric adenosine acid (ATP), the participation of coenzyme A (CoA) and redox systems at the cellular level through the H-shaped passages of nicotin-amino-dinucleoid ($NAD \xleftrightarrow[H^+,\ e^-]{} NADH$) respectively nicotine-amide-dinucleotide-phosphate ($NADP \xleftrightarrow[H^+,\ e^-]{} NADPH$).

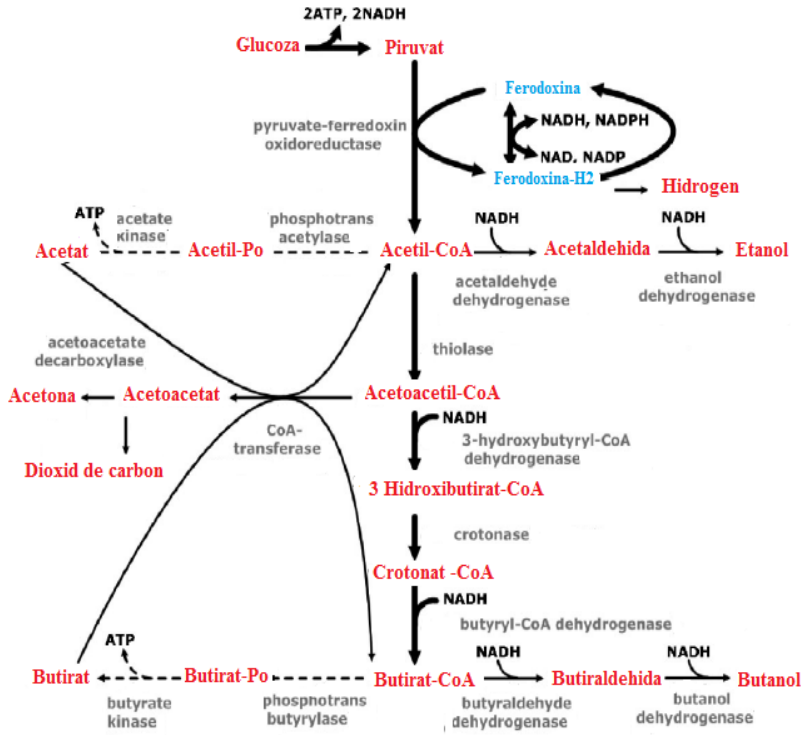

Figure 2.9 Scheme of the metabolic process of obtaining EBA solvents with the Acetobutylicum Clostridium system (with dotted line reactions from the acidogenic stage, with continuous line reactions from the solventogenic stage)

If it is accepted that the passage of glucose (reactant) and all cellular metabolites through the cell membrane is rapid then the enzyme processes in the cell determine the overall speed of the process. It is accepted that each of the 17 enzyme reactions follows a Michaelis Menton kinetic [38]. The kinetic model in the cell is expressed by the relationship (2.8), where c_{Si} is the concentration of species i (in red in Figure 2.9) involved in the process, and $v_{Rmax\,i}$ and k_{Mi} are the maximum speed characteristic of the enzyme reaction and the Michaelis Menton constant respectively.

$$v_{R\,i} = -\frac{dc_{S\,i}}{d\tau} = \frac{v_{Rmax\,i} c_{S\,i}}{k_{M\,i} + c_{S\,i}} \quad i = 1,..17\ (glucose, pyruvat, \ldots butanol) \tag{2.8}$$

Fermentation requirements. Regarding the requirements of fermentation, it should be noted that they may be influenced by the processing of the materials before fermentation and by the post fermentation processing of the fermented environment [39]. With regard to the fermentation itself, it has been found that the use of the substrate as excess carbon together with the limitation of nitrogen (proteins) in the fermentation environment is necessary to achieve high levels of solvents production.

Since the role of the composition of the culture medium in the transformation of the carbon substrate into solvents must be highlighted, selective collection of data from the literature [42-46] and some of its own was gathered, where it was intended to show the influence on this transformation of glucose concentration (main carbon source and at the same time reporting source (comparison) to other main sources), butyric acid (secondary carbon source, desirable to be added according to Figure 2.9), C/N ratio (N is the source of

nitrogen in cell protein synthesis) and temperature. Systematized data refer to the case where the bacterial system was of the type Clostridium Acetobutylicum (in fact this bacterial system has several forms but have almost all the same behavior) and when for each combination of process factors the preparation of the inocul was almost similar, the pH was kept between 4.8 and 5.8, and the standard composition of the culture medium was according to the data in Table 2.1.

Table 2.1 Standard composition for EBA fermentation medium with Clostridium Acetobutylicum

N.c	Name of compound	u.m	Value
1	Inocul clostridium	mL/L	75
2	Glucose	g/L	50
3	Butyric acid	g/L	5
4	Ammonium acetate	g/L	2
5	Triptona	g/L	5
6	Yeast extract	g/L	2
7	Magnesium sulfate	g/L	0.3
8	Heptahydrate iron sulphate	g/L	0.001

The experimental orthogonal plan of order 2 [5] highlights the influence of factors interaction as well as factors squares on the three responses considered, respectively: butanol concentration (c_B), the ratio between butanol and acetone concentration ($r_{BA} = c_B/c_B$) and the total concentration of solvents ($c_{TS} = c_B + c_A + c_E$).

Substrate for fermentation. In Figure 2.9, up to the fermentation phase where ethanolic fermentation is replaced by butanolic fermentation, it has been shown how complex the process of obtaining fermentable sugars is, starting from vegetable residues. This makes the price of the butanol that would come along the path of generation 3 biofuel still high. The fermentation substrate in EBA technology is linked to the bacterial system used. There are assessments, including economic [50], which show that the use of the Strain of Clostridium Beijerinckii, on hydrolysed sugars from corn flour, give a good productivity to butanol, somewhere between 0.4 - 0.5 g butanol/g glucose equivalent, at a price estimated at the level of the year 2000, of 0.3 - 0.35 $/kg butanol crude (unseparated). We show here that we can integrate the biodiesel technology with the EBA fermentation technology in which the glycerin, by-product from biodisel, was successfully used as a partial or main fermentation substrate [51] where it reached a productivity of 0.35 to 0.45 g biobutanol/g glycerin.

Butanol toxicity to the microorganism system. One of the particularly important problems in EBA fermentation is the toxicity of solvents to the bacterial system. Of the three solvents it is certain that only butanol is toxic to cells during fermentation with clostridian bacteria.

At the forefront of solutions to eliminate the problem of butanol toxicity on the Clostridium bacterial system are the technological procedures that are called generic in situ recovery, i.e. procedures for removing butanol from the fermentation medium in one way or another [58,59].

Considerations on the use of genetic engineering in EBA synthesis. In 2001 the complete sequence of the genome of Clostridium Acetobutylicum was published [60]. Without going into detail, it is shown that the objectives of genetic and metabolic engineering are to obtain clostridian bacterial systems leading to a higher productivity in

butanol, a very good tolerance to butanol (not to affect bacterial growth up to 40 g/L butanol in the culture medium), to the possibility of using them for as much substrate base as possible. It is obvious that genetic engineering must act on the gene system and their combination for both those participating in the acidogenic phase of fermentation and those specific to the state of RNA in the solventogenic phase. For the purposes of the use of a rigid substrate such as cellulose in the bacterial system, it is shown how in Clostridium Acetobutylicum the gene responsible for the consumption of cellulose, Clostridium Cellulovorans, respectively the gene encoding the protein assembly of Clostridium Celluloticicum and Clostridium Thermocellum, was introduced. This resulted in the consumption of non-hydrolysed cellulose in EBA synthesis, even though the yield was decreased [61].

Solvent recovery and in situ processes. The high cost of recovering the product(s) is another issue of great importance in most biotechnology-based manufacturing, including fermentation. In this case solvents, acetone, butanol and ethanol can obviously be separated by traditional distillation. This process suffers from the fact that it has a high cost due to the low concentration of solvents in the processing medium. In order to solve this problem of the price of distillation and also to respond to the problem of toxicity of butanol to the bacterial system, it has been passed, not only experimentally, to what is called the separation of solvents in situ, as they form. The level of butanol concentration in the fermentation medium shall be controlled by removing solvents from it so that it is not in the toxicity range. At the same time this concentration level of butanol in the environment corresponds to high productivity values in solvents. A first process [62 - 65] is that of gas stripping of solvents (Figure 2.15).

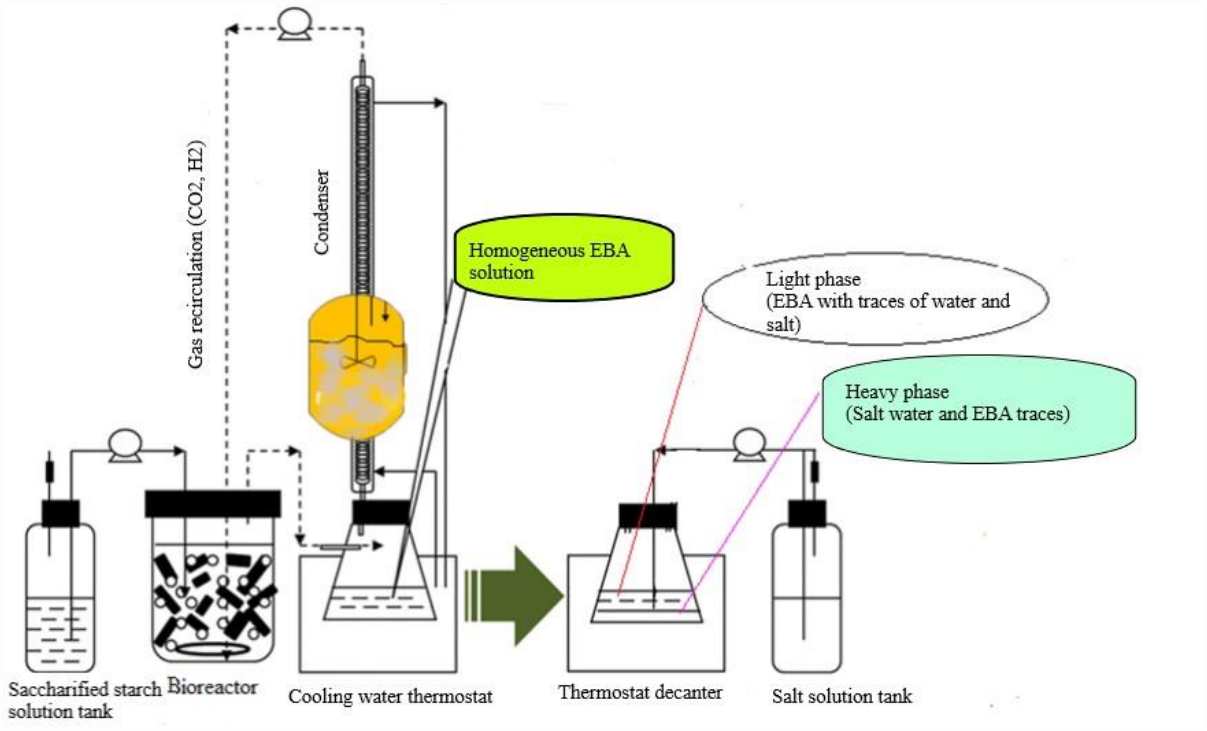

Figure 2.15 Coupling of EBA fermentation with gas drive of solvents and separation salification

Another process highly studied and applied at all levels of process scales-up is the coupling of EBA fermentation with pervaporation [66-68]. Because the pervaporation

membranes are sensitive to cell medium clogging between the fermentation bioreactor and the pervaporation module, an ultrafiltration module (Figure 2.16) has been introduced into this process that protects the pervaporation module from clogging and additionally on the cell recirculation pathway so that the level of cell concentration in the bioreactor can be a desired one.

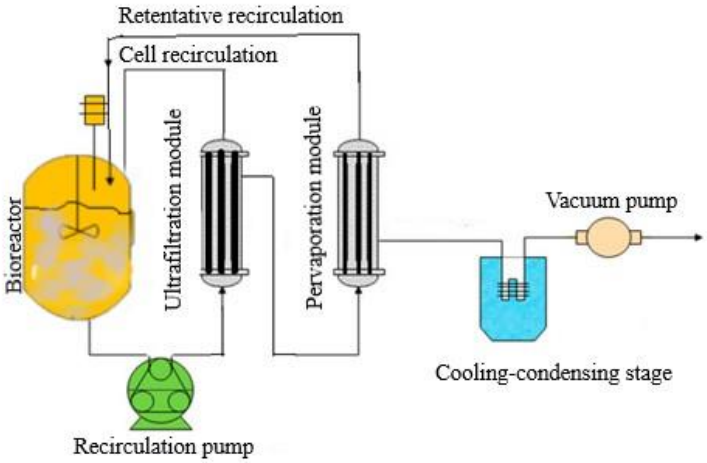

Figure 2.16 Coupling EBA fermentation with ultrafiltration and pervaporation with selective solvent separation membrane

Liquid-liquid extraction is another effective technique for removing acetone, butanol and ethanol solvents from the fermentation medium. Schematically the process is shown in Figure 2.17.

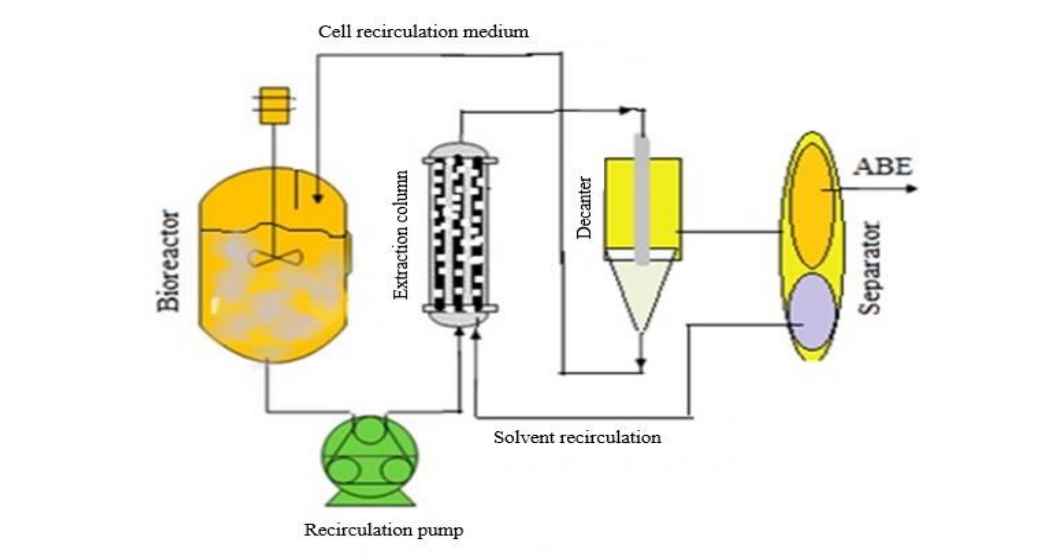

Figure 2.17 Coupling EBA fermentation with liquid-liquid extraction

Liquid-liquid extraction has critical problems, such as the toxicity of the extraction solvent for the bacterial cell and also the emulsifying of the solvent in the fermentation

medium or vice versa in the extraction solvent. There are solutions to these problems. One solution would be to interscale between the bioreactor and the extractor (Figure 2.17) an ultrafiltration module so that the extraction is worked with a medium without the presence of bacterial cells. The same problem can be solved by using a membrane extractor in which the fermentation medium is separated from the extraction solvent by a permeable membrane.

Table 2.5 provides a series of data on the effectiveness of the use of the three techniques for in situ separation of EBA fermentation solvents.

Table 2.5 Data on comparing the performance of integrated fermentation processes with EBA recovery

N.c	Type of bioreactor	Conc. substrate g/L	Conc. EBA g/L	Productivity g_{ABE}/ (L/h)	Yield g_{ABE}/ $g_{substr.}$	Source
1	Batch	60-70	20-24	0.32-0.35	0.4-0.42	70,73,74
2	Fed batch	70-80	25-28	0.35-0.4	0.41-0.43	75
3	Batch with gas stripping	100-110	25-35	0.51-0.55	0.43-0.47	74 76
4	Fed batch with gas stripping	140 -150	35-45	0.9-1.05	0.45-0.48	76,77
5	Batch with pervaporation	70 -75	30-35	0.5-0.53	0.42-0.44	78,79
6	Fed batch with pervaporation	120-130	35-38	0.89-0.95	0.45-0.48	80
7	Batch with extraction	100 -110	30-35	0.53-0.55	0.46-0.48	70,81
8	Fed batch with extraction	100-120	36-39	0.75-0.85	0.45-0.48	81,82

2.6.2 General aspects regarding the production of bioethanol (fermentation ethanol)

Ethanol is also a safer alternative to methyl-third-butyl-eter (MTBE), the most common additive used in gasoline to ensure a cleaner combustion.

However, the cost of ethanol as an energy source for engines is relatively high compared to fossil fuels. A strong increase in ethanol production using current starch(s) technology of corn (or other cereals) may not be practical for small countries, as ethanol maize production competes on the agricultural land market, where there are limitations imposed by food and feed production. Forcing this market would lead to higher food prices and therefore putting countries, particularly in the third world, in an extreme position.

The solution is to develop the technology of bioethanol of generation 3, which based on biomass (straw, stems, foliage, grass, sawdust, wood chips, forest waste, specialized crops, etc.) so that the manufacturing price is competitive with that of fossil fuels.

Bioethanol from corn flour. As a description, from the point of view of biochemical reactions, we show that we have here, in what is called the saccharification phase, respectively the fermentation phase, a series of enzyme reactions that convert amylose and amylopectin, from corn flour, into maltose and then into glucose, followed by the biochemical processes characteristic of alcoholic fermentation. Figure 2.18 schematically shows these reactions, numbered (2.17) at (2.21).

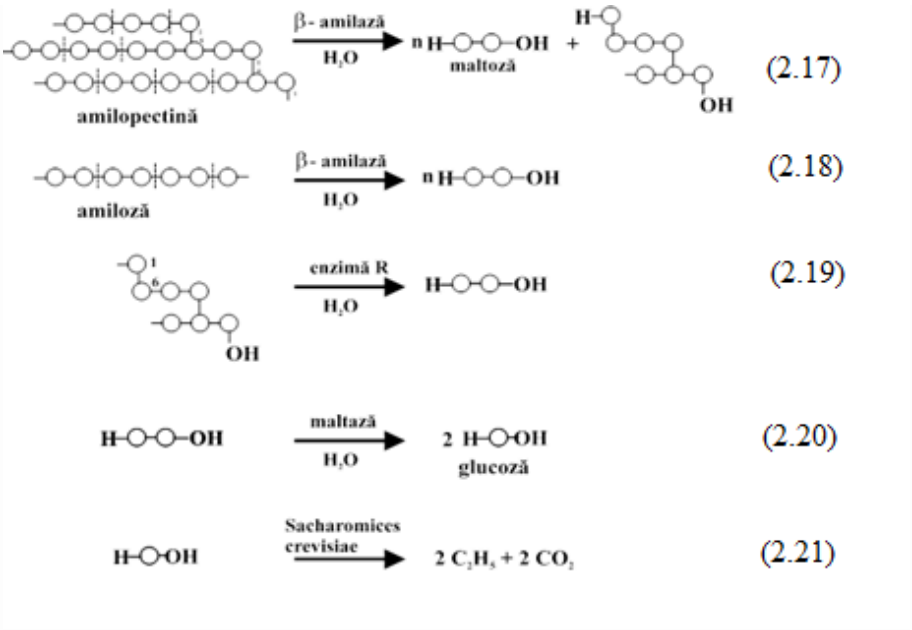

Figure 2.18 Biochemical reactions to obtain biobutanol from starch

The saccharification part of the starch is carried out, as mentioned above, by means of enzymes. One of the sources of enzymes is malt.

Due to its specificity, as shown by the reactions (2.17) ÷ (2.19), some enzymes will hydrolyze the bond 1–4 of the glucose molecules in starch, others will produce the attack on the 1–6 bonds of the same structure (Figure 2.19).

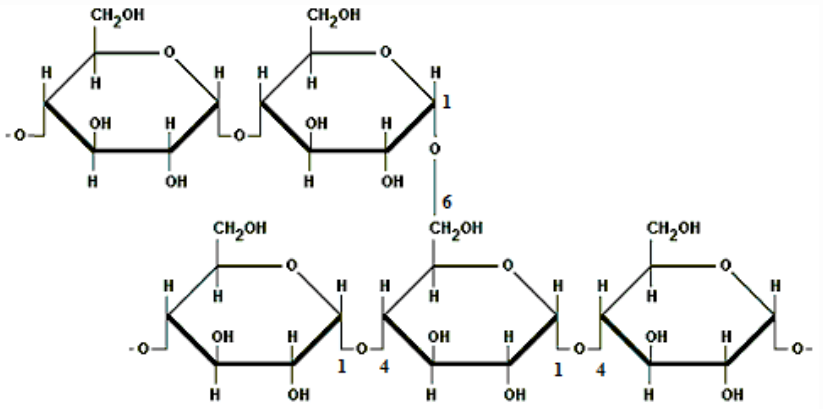

Figure 2.19 Fragment of an amylopectin macromolecule with highlighting of hydrolysable bonds (1-4), (1-6)

Among the enzymes attacking the bonds 1-4, 1-6 of the characteristic structure of the starch is mentioned amylase α and amylase β.

Figure 2.20 shows the diagram of the main operations in case the saccharification enzymes (α-amylase and β-amylase) are brought only from malt.

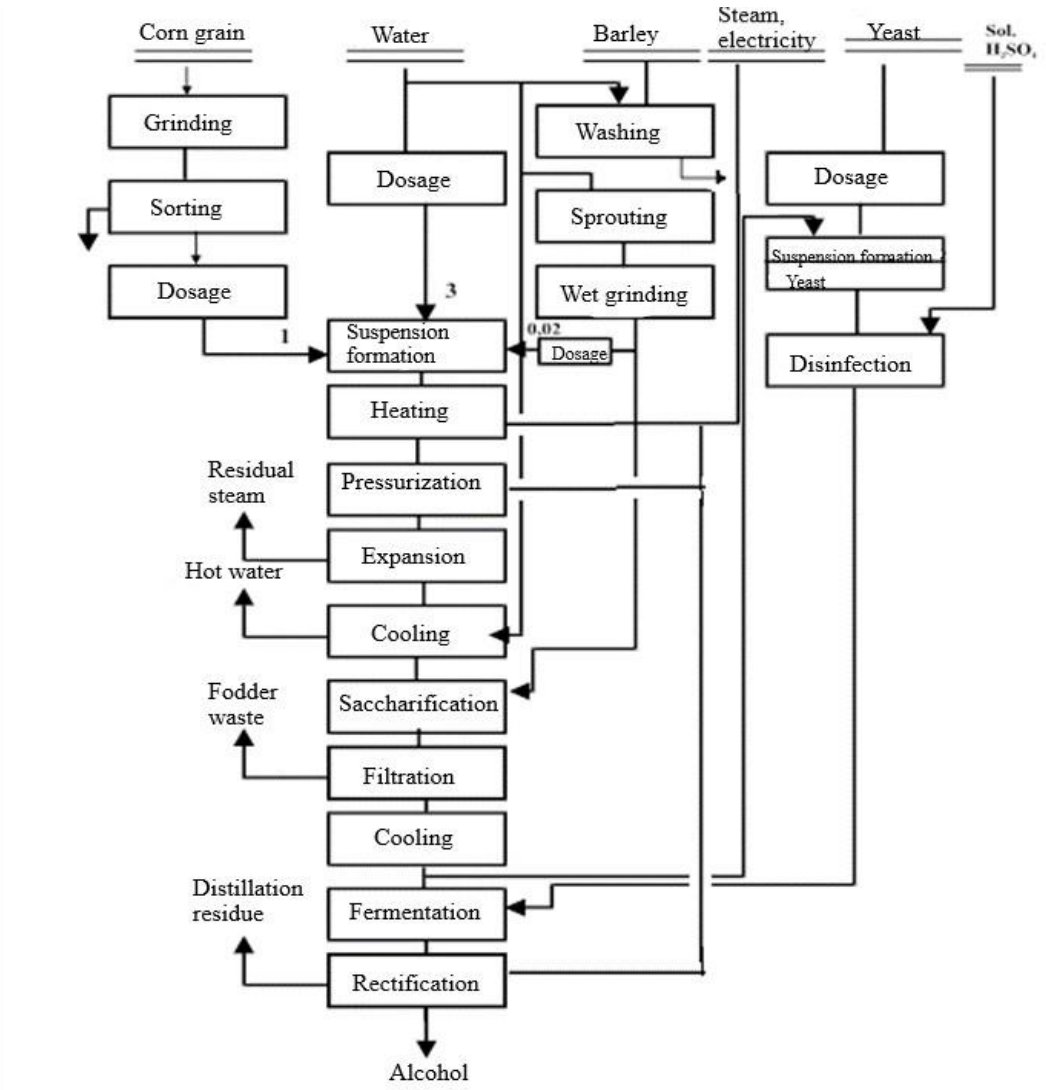

Figure 2.20 Scheme of main operations in the production of bioethanol from corn flour

The two processes in the main operations scheme can be characterized by the generalized expression given by the relationships (2.22) and (2.23). On this basis, a simple procedure for estimating specific consumptions can be developed.

$$[C_{12}H_{22}O_{11}]_n + nH_2O \xrightarrow{saccharification} 2nC_6H_{12}O_6 \quad (2.22)$$

$$C_6H_{12}O_6 \xrightarrow{fermentation} 2C_2H_5OH + 2CO_2 \quad (2.23)$$

From the reaction (2.23), after small calculations, it is found that 1 kg of ethyl alcohol results from 1,956 kg of glucose, at the same time from the reaction (2.23) it is deduced that 1 kg of glucose (actually 1 kg fermentable species) comes from 0.94 kg of starch. From the two observations it is concluded that 1 kg of ethyl alcohol should result from 1,837 kg starch i.e. the theoretical specific consumption of starch is 1,837 $kg_{starch}/kg_{ethanol}$. The actual specific consumption of starch and therefore the specific consumption of corn flour is much higher. Table 2.8 presents the calculation of this consumption considering that the fermentation

reaction is carried out with processing yields of 0.7, 0.8 and 0.9, and the saccharification reaction has yields of 0.5, 0.7 and 0.9. For corn flour was considered composition: 80% starch, 8% protein, 8% water and 4% others.

Table 2.8 Determination of specific consumption of corn flour

η_{ferm}	0,7			0,8			0,9		
η_{zah}	0,5	0,7	0,9	0,5	0,7	0,9	0,5	0,7	0,9
$c_{s\ amid}$ kg_{amd}/kg_{alc}	5,25	3,75	2,92	4,59	3,28	2,55	4,08	2,91	2,26
$c_{s\ făină}$ = $kg_{făină}/kg_{alc}$	6,56	4,68	3,64	5,73	4,1	3,18	5,10	3,64	2,84

In addition to corn flour as direct raw materials, water is also used, barley malt and beer yeast, which are dosed according to the unit of mass of the main raw material (corn flour).

Important kinetic processes for obtaining bioethanol from corn flour. When obtaining bioethanol from corn flour there are 3 major kinetic processes, namely: i) the gelatinization of starch from the flour particle, ii) the saccharification of gelatinized starch and respectively iii) the fermentation of sucrose. The first process is a physico-chemical process, the other two being biochemical processes.

2.6.3 Fermentation biogas

Anaerobic digestion of organic matter is a well-spread process in nature.

Biogas is a mixture of methane and carbon dioxide, with some contamination of hydrogen sulfide, mercaptans, ethane, etc. Methane content varies from 55 to 90% volume, depending on the nature and content of the substrate, the method of digestion and many other factors.

Anaerobic digestion is also a convenient technology for the active use of sludge from depollution stations and the treatment of waste in the food, cellulose and paper industries, as well as in the treatment of household waste. Anaerobic digestion with biogas production is a catalyzed process of enzymes produced by various bacterial microorganism that hydrolyze organic macromolecules (carbohydrates and proteins) to oligosaccharides and peptides and hence through the phases of acidogenesis, acetogenesis and methanogenesis to the main end products, methane and carbon dioxide [104].

Considerations on the elementary processes in the production of biogas. As with the two fermentations, and in particular as in the case of obtaining EBA solvents, we have a multi-phase process, as stated above.

In Figure 2.22 we show that we can consider two large phases, namely hydrolysis, when small molecules are obtained by hydrolytic rupture of large ones, respectively fermentation, when small molecules enter into a complex biochemical process distributing 76% to the path of superior organic acid biosynthesis (the sequence being called acidogenesis), 20% to the path of acetic acid (sequence called acetogenesis) and 4% to the path of hydrogen and formates (the sequence is called dehydrogenation).

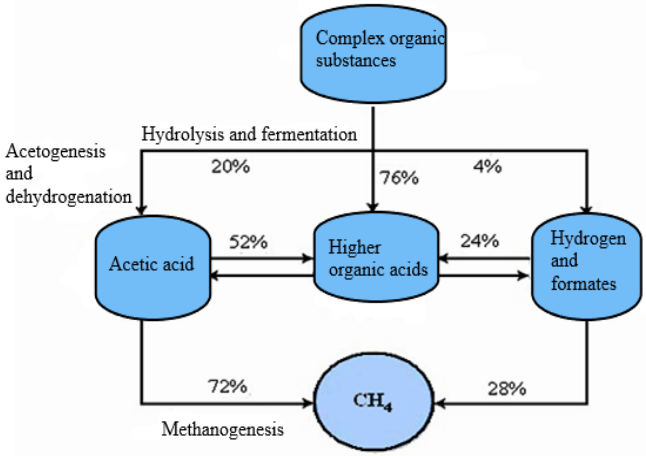

Figure 2.22 Percentage distribution of the circulation of hydrolysates of organic species when obtaining biogas

Between the states of acetic acid-superior organic acids-hydrogen and formates are transitions to balance with the proportions written on Figure 2.22. Methane generated in the last phase, called methanogenesis, comes only from the state of acetic acid (acetate) and that of hydrogen and formates.

In order to translate into chemical reactions, the above mentioned biochemical processes, the initial complex organic material is considered to be cellulose. The reactions or reaction sets below can be written:

Hydrolysis: $(C_6H_{10}O_5)_n + nH_2O \underset{e,m}{\longrightarrow} nC_6H_{12}O_6$ (2.35)

Alcoholic fermentation: $C_6H_{12}O_6 \underset{d}{\rightarrow} CH_3CH_2OH + CO_2$ (2.36)

Propionic conversion: $C_6H_{12}O_6 + 2H_2 \underset{e,m}{\leftrightarrow} 2CH_3CH_2COOH + 2H_2O$ (2.37)

Acetogenesis reactions:

$$2CH_3CH_2COO^- + 3H_2O \underset{e,m}{\overrightarrow{\leftrightarrow}} CH_3COO^- + H^+ + HCO_3^- + 3H_2$$ (2.38)

$C_6H_{12}O_6 + 2H_2O \underset{e,m}{\longrightarrow} 2CH_3COOH + 2CO_2 + 4H_2$ (2.39)

$2CH_3CH_2OH + O_2 \underset{e,m}{\longrightarrow} 2CH_3COOH + H_2O$ (2.40)

$2HCO_3^- + 4H_2 + H^+ \underset{e,m}{\longrightarrow} CH_3COOH + 4H_2O$ (2.41)

Methanogenesis reactions:

$CH_3COOH \underset{b,mt}{\longrightarrow} CH_4 + CO_2$ (2.42)

Another way of generating methane by other methanogenic bacteria than those involved in the reaction (2.42) is that of formiate (formic acid) resulting from the decomposition by some enzymes of glucose or propionic acid (Figure 2.22). In this case reactions (2.43) and (2.44) occur.

$HCOOH \underset{e,m}{\longrightarrow} H_2O + CO_2$ (2.43)

$$CO_2 + 4H_2 \underset{e,m}{\longrightarrow} CH_4 + 2H_2O \quad (2.44)$$

Biochemical activity of bacteria and implicitly biogas productivity is confirmed to be high in two temperature ranges, i.e. at temperature between 30°C and 40°C (fermentation is known as mesophilic methanogenic fermentation), i.e. between 50°C and 60°C (thermophilic methanogenic fermentation field). The mesophilic regime between 32°C and 35°C is sufficiently reliable for stable and continuous methane production. Biogas produced outside this temperature range is rich in carbon dioxide and cannot be direct fuel.

Microorganisms (bacteria) in the production of biogas. Different methanogenic strains are responsible for these parallel and competitive processes expressed by all reactions (2.35)÷(2.44). Here notations such as, $\underset{e,m}{\longrightarrow}$ want to show that the reaction is catalyzed by enzymes produced by microorganisms. The balance between the decarboxylation of acetic acid and the reduction of carbon dioxide is important for the methane content of the resulting biogas. If only the decarboxylation of acetic acid occurs then a biogas with methane and carbon dioxide with equal molar fractions should result, the relationship (2.42). A higher methane content in biogas means that reducing carbon dioxide, the relationship (2.44), is as important as the participation in the global process.

Selective bibliographic references

[5]. Dobre T., Sanchez J.M., Chemical Engineering Modeling Simulation and Similitude, Cap: Why Modeling, Wiley VCH, 2007

[30]. Campbell C. J., Laherrere H., The end of cheap oil, Scientific American, 3, 78–83, 1998

[31]. Jones D.T., Woods D.R., Acetone–butanol fermentation revisited, Microbiol Rev., 50, 484–524, 1986

[36]. Herman A.N., Kim J.S., Li S. J., Cai W., Koshino H., Zhang W., The industrial anaerobe Clostridium acetobutylicum uses polyketides to regulate cellular differentiation, Nature Communications, 8, Art No:1514, 2017

[37]. Hartmanis M.G.N., Gatenbeck S., Intermediary metabolism in Clostridium acetobutylicum: Levels of enzymes involved in the formation of acetate and butyrate, Appl. Microbiol. Biotechnol., 47, 1277–1283, 1984.

[39]. Qureshi N., Blaschek H.P., Evaluation of recent advances in butanol fermentation, upstream, and downstream processing, Bioproc. Biosys. Eng., 24, 219–226, 2001

[42]. Fond O., Matta-Ammouri G., Petitdemange H., Engasser J.M., The role of acids on the production of acetone and butanol by Clostridium acetobutylicum Appl. Microbiol. Biotechnol. 22 , 3, 195–200, 1985

[43]. Jones T. D., Woods. R. D., Acetone-butanol fermentation revisited, Microbiological Reviews, 50, 4, 484–524, 1986.

[44]. Khamaiseh I. E., Hamid A. A., Abdeshahian P., Mohtar Y., Kalil S. M., Enhanced butanol production by Clostridium acetobutylicum NCIMB 13357 grown on date fruit as carbon source in P2 medium, The Scientific World Journal,Vol.2014, Paper ID 395754, 2014

[45]. Al-Shorgani N. K. N., Shukor H., Abdeshahian P., Kalil S. M., Mohtar Y., Hamid A.A., Enhanced butanol production by optimization of medium parameters using Clostridium acetobutylicum YM1, Saudi Journal of Biological Sciences 25, 1308–1321, 2018

[46]. Singh V., Haque S., Niwas R.., Srivastava A., Pasupuleti M., Tripathi M. K. C., Strategies for fermentation medium optimization: An in-depth review, Frontiers in Microbiologies, 7, Papers 2087, 2017
[50]. Qureshi N., Blaschek H.P., ABE production from corn: A recent economic evaluation, J Ind. Microbiol. Biotechnol., 27, 292–297, 2001
[51]. Andrade J.C., Vasconcelos I., Continuous cultures of Clostridium acetobutylicum: Culture stability and low-grade glycerol utilization, Biotechnol. Lett., 25, 121–125, 2003
[58]. Lee S.Y, Lee D-Y, Kim T.Y., Systems biotechnology for strain improvement, Trends Biotechnol., 23, 349–358, 2005
[59]. Ohreac Sandu B., Dobre T., Pârvulescu O., Danciu T., Integrations of ABE synthesis with their recovery by gas-stripping, Rev. Chim. (Bucharest), 65,5, 581-588, 2014
[60]. Nolling J., Breton G., Omelchenko M.V., Makarova K.S., Zeng Q., Gibson R., Lee H.M., Dubois J., Qiu D., Hitti J., Wolf Y.I., Tatusov R.L., Sabathe F., Doucette-Stamm L., Soucaille P., Daly M.J., Bennett G.N., Koonin E.V., Smith D.R., Genome sequence and comparative analysis of the solvent-producing bacterium Clostridium acetobutylicum. J Bacteriol., 183, 4823–4838, 2001
[61]. Perret S., Casalot L., Fierobe H.P., Tardif C., Sabathe F., Belaich J.P., Belaich A., Production of heterologous and chimeric scaffoldings by Clostridium acetobutylicum ATCC 824, J. Bacteriol., 186, 253–257, 2004
[62]. Qureshi N., Maddox I.S., Friedl A., Application of continuous substrate feeding to the ABE fermentation: relief of product inhibition using extraction, perstraction, stripping, and pervaporation. Biotechnol Prog 8:382–390, 1992
[63]. Vrana L. D., Meagher M. M., Hutkins W.R., Duffield B., Pervaporation of model acetone-butanol-ethanol fermentation product solutions using polytetrafluoroethylene membranes, Separation Science and Technology, 28, 13-14, 2167-2178, 1993
[64]. Ezeji T.C., Qureshi N., Blaschek H.P., Production of butanol by Clostridium beijerinckii BA101 and in situ recovery by gas stripping, World J. Microbiol. Biotechnol., 19, 595–603, 2003
[65]. Xue C., Zhao J., Lu C., Yang S., Bai F., Tang I., High-titer n-butanol production by Clostridium acetobutylicum JB 200 in fed-batch fermentation with intermittent gas stripping, Biotechnol Bioeng., 109, 2746–56, 2012
[66]. Qureshi N., Meagher M. M., Huang J., Hutkins W. R., Acetone butanol ethanol (ABE) recovery by pervaporation using silicalite–silicone composite membrane from fed-batch reactor of Clostridium acetobutylicum, Journal of Membrane Science, 187 93–102, 2001
[67]. Liu P. G., Hou D., Wei W., Xiangli J. F., Jin Q. W., Pervaporation separation of butanol–water mixtures using polydimethylsiloxane/ceramic composite membrane, Chin. J. Chem. Eng.1940–44. (2011)
[68]. Hecke W., Van Hofmann, T., De Wever H., Pervaporative recovery of acetone-butanol-ethanol (ABE) during continuous cultivation: Enchament of performance, Bioresource Technology, 129, 421–429, 2013
[104]. Trică B., Pârvulescu O.C., Dobre T., Al Janabi A.A.A., Răducanu C., Patrichi C., Modelling of Ethanol Fermentation Coupled with Product Recovery by Pervaporation, Rev. Chim. (Bucharest), 68, 11, 2708-2715, 2017

CHAPTER 3
Coupling separation with membranes with alcoholic fermentation

In many cases the coupling of processes in the sense of introducing separation into the field of the chemical or biochemical process of a given synthesis, has led to spectacular results, of great industrial interest.

3.2 PVA-BC pervaporation membranes on the support

Figure 3.2 shows the manufacturing stages and the results of this process, where the thin layer of the membrane is applied to the external support of the ceramic tube.

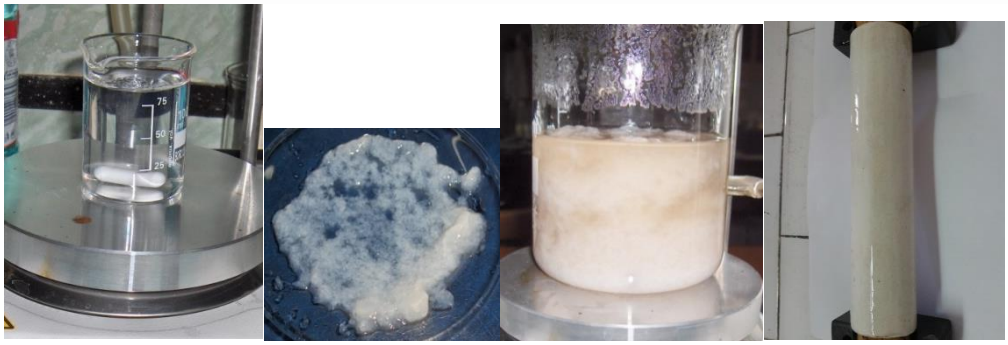

(a) *(b)* *(c)* *(d)*

Figure 3.2 The stages of preparation of rigid PVA-BC membrane on ceramic support:
PVA solution (a), wet grinded BC (b), PVA-BC mixture with glutaraldehyde (c), rigid membrane (d)

3.2.1.3 Pervaporation tests

Pervaporation experiments involving this rigid membrane were carried out in a laboratory equipment by having the membrane tube placed in a closed batch glass, which can be placed under vacuum. An image of this equipment (pervaporation unit) is attached to its schematic in Figure 3.3, where it is shown the complete laboratory equipment.

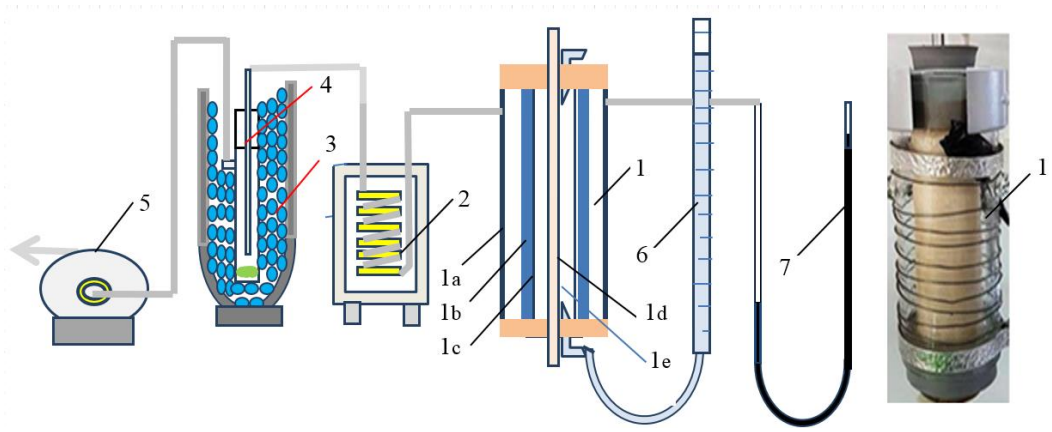

Figure 3.3 Laboratory equipment for permeation studies with rigid membranes on external surface of one ceramic tube (**1**-pervaporation unit, **2**-electric cooler (5-6^{0}C), **3**-Dewar vessel with crushed ice, **4**-steam condenser with central tube, **5**-vaacum pump, **6**-precision burette for permeate flow rate measurement, **7**-mercury manometer, **a**-glass tube, **b**-PVA-BC membrane, **c**-ceramic support, **d**–tube for heating processed liquid, **e**–processed etanol-water mixture)

Operating of pervaporation test. The PV experiments have been carried out at different temperatures, 30ºC, 40ºC, 50ºC and respectively 60ºC. In order to achieve this, the hot water

from the thermostat bath crosses through the PV system, the thermostat containing a thermometer to set the temperature required. Pressure of 14, 24 and 28 cm Hg has been used inside of the pervaporation chamber, by controlling the vacuum pump.

Table 3.1 Data showing some results of laboratory experiments. Experimental data

N	c_{Etoh}%	n_{Df}	Conditions		V mL	Pervaporation interval for a run, s				
			t °C	P mmHg		1	2	3	4	n_{Dp}
First membrane (12 PVA:6 raw BC, r =2)										
5	48	1.3580	60	140	2	58	50	46	56	1.3597
7	48	1.3580	40	280	2	66	63	66	72	1.358
8	24	1.3445	60	280	2	61	48	45	45	1.356
9	24	1.3445	60	140	2	45	35	17	10	1.351
Second membrane (12PVA:12 raw BC, r = 1)										
13	24	1.3445	60	240	2	28	42	43	42	1.333
14	24	1.3445	40	240	2	39	39	39	40	1.337
15	48	1.3580	60	140	2	38	28	25	25	1.3425
21	72	1.3615	40	240	2	90	90	90	88	1.335
Third membrane (12 PVA:18 raw BC, r = 0,66)										
23	72	1.3615	60	240	2	99	80	70	71	1.336
26	72	1.3615	40	240	2	97	97	98	97	1.336
29	48	1.3580	60	140	2	61	54	51	50	1.335
33	24	1.3445	40	240	2	49	50	55	56	1.333

3.2.1.5 Results and discussions

In order to analyze the membrane structure, we start by observing the FTIR spectra for first (PVA/BC =2), second (PVA/BC =1) and third (PVA/BC =0.66) membranes, which were used in the pervaporation experiments.

Due to the fact that the FTIR spectra analyzes only the vibration of the molecular groups, it is not expected to have many differences between the three membranes spectra, which differ only in BC content, as shown in Figure 3.5. For a better analysis of this statement, the FTIR spectra for BC (Figure 3.6) and PVA film together with crosslinked PVA film (Figure 3.7) are provided. Also, it is expected to have important differences between the spectra of our membranes and between the characterizations of the PVA reticulated membrane (Figure 3.7) and BC (Figure 3.6). It underlines that the main component of the membrane is PVA.

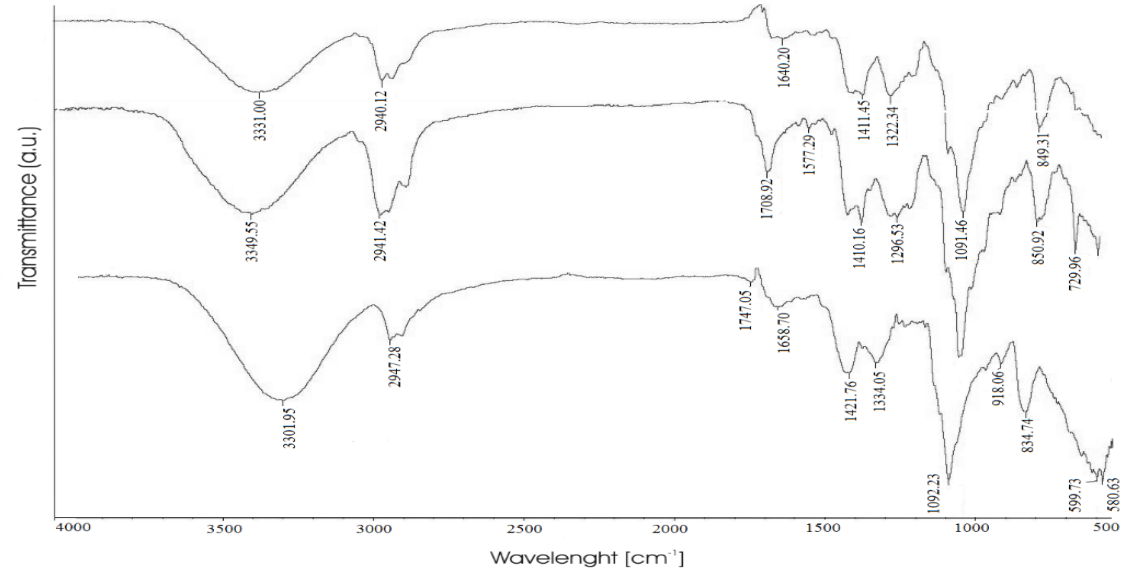

Figure 3.5 FTIR transmittance spectra for first (top), second (middle) and third (bellow) composite membranes after preparing and drying at 90 ^{0}C

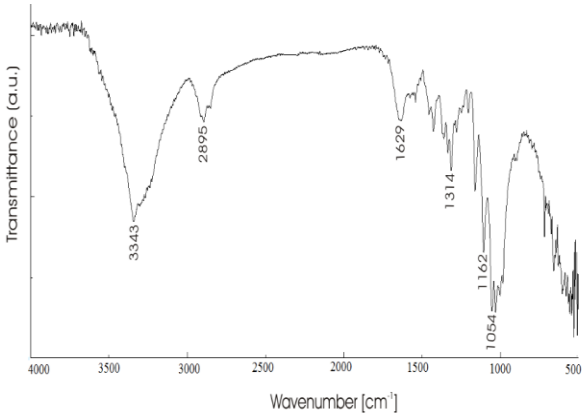

Figure 3.6 FTIR Transmittance spectrum of BC for composite membranes synthesis

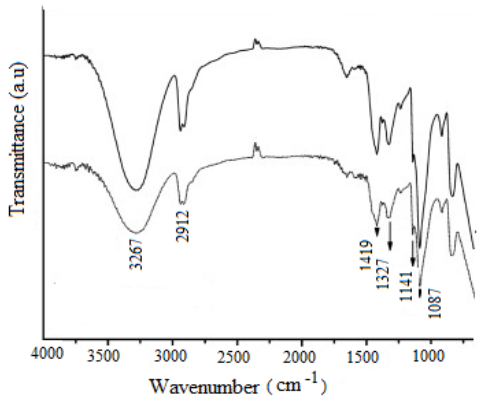

Figure 3.7 FTIR transmittance spectra for PVA (top) and glutaraldehyde reticulated PVA (bellow)

We identify 7 common peaks for BC and cross-linked PVA (3267 cm^{-1}, 2912 cm^{-1}, 1629 cm^{-1}, 1419 cm^{-1}, 1327 cm^{-1}, 1141 cm^{-1} and 1087 cm^{-1}) which are found, more or less easily displaced, due to the stiffening of the structure, in the FTIRs of our three membranes.

When counting we find that in the spectra of our membranes, we have 7 peaks for the membrane with the ratio PVA/BC 2, 9 peaks for the membrane where this ratio is 1, respectively 11 peaks for the membrane where this ratio is 0.66. If we look comparatively to the FTIRs of these three membranes, we identify that as the concentration of BC in the

membranes increases, new peaks appear (1577 cm^{-1} and 729 cm^{-1} for second membrane compared with the first; 918 cm^{-1}, 599 cm^{-1} and 580 cm^{-1} for third membrane compared with the second). We notice in our membranes the slight displacement of the peaks characteristic to cross-linked PVA and BC, together with the appearance of new peaks, specific to these membranes, several of them being connected to the increase of the concentration of BC in the membrane. It can be concluded that the three membranes have similar structures, which differ depending on their BC content. It is thus expected that in pervaporation of some organic solutions containing water, such as the ethanol-water mixture, the three membranes will behave differently. It should be added that the preservation, in the structures of these membranes, of the characteristic PVA and BC bonds, allow us to consider that they preserve the facilitated water transport capacity, existing in PVA and BC.

For the process of membranes synthesis, in Figure 3.8, by mean of optic images, is shown the macroscopic distribution of disintegrated BC fibrils in PVA solutions. It is observed the BC distribution as micro agglomerates, having a concentration consistent with that of the initial BC content.

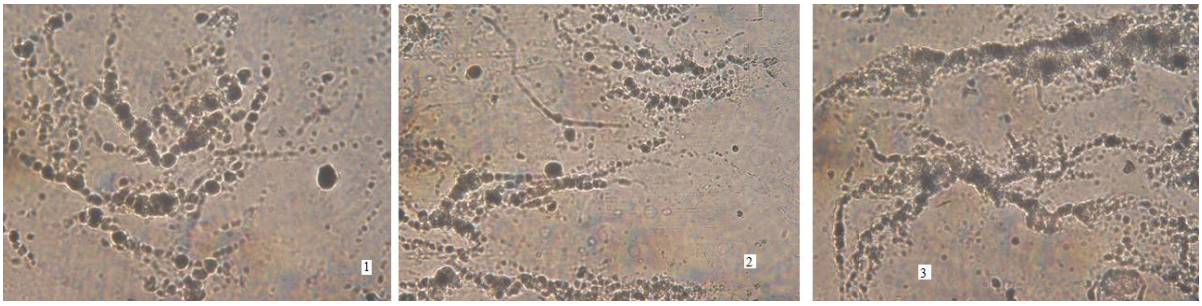

(1) **(2)** **(3)**

Figure 3.8 Optic microscope images (X10) of first (1), second (2) and third (3) PVA-BC mixture before the start of membrane reticulation

SEM images, presented in Figure 8, at a resolution of 20 μm, show a composite membrane in which the compact PVA film is furrowed, almost neatly, by BC fibers having less than 2 μm. It can be appreciated that the density of fibrils in the films is proportional with the BC content used in their preparation.

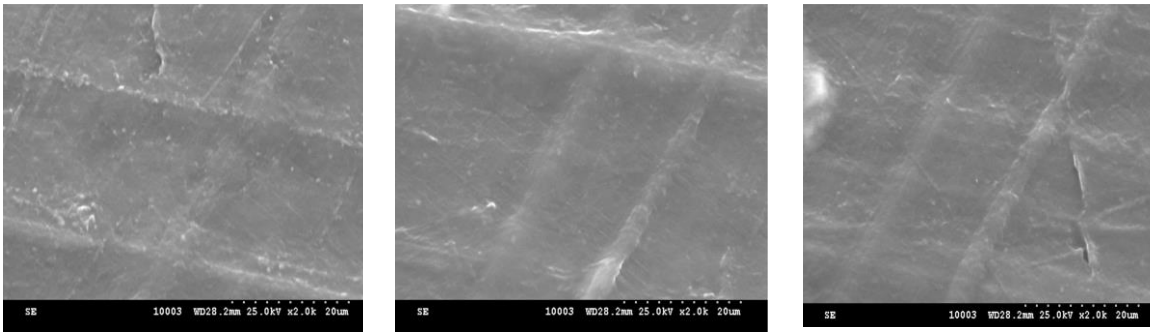

(a) **(b)** **(c)**

Figure 3.9 SEM images of rigid film of first (a), second (b) and third (c) membranes

Table 3.2 Processed experimental data for the dependence of total permeate flux (N_A) and membrane selectivity for water versus process parameters (case of second membrane)

n	c_{Etf} (%)	x_3	Temperature and pressure				N_A (kg/m^{2}h)	c_{Etp} (%)	$\alpha_{w/et}$
			t (°C)	x_1	p (kPa)	x_2			
1	24	-1	40	-1	18.666	-1	0.182	3.18	8.6
2	24	-1	60	1	18.666	-1	0.203	2.92	9.5
3	24	-1	40	-1	31.998	1	0.195	5.24	4.7
4	24	-1	60	1	31.998	1	0.218	4.92	5.1
5	72	1	40	-1	18.666	-1	0.089	20.63	8.9
6	72	1	60	1	18.666	-1	0.097	24.71	6.8
7	72	1	40	-1	31.998	1	0.092	13.95	14.8
8	72	1	60	1	31.998	1	0.112	11.50	18.8
9	48	0	50	0	20.333	0	0.151	8.30	9.2
10	48	0	50	0	20.333	0	0.148	8.05	9.6
11	48	0	50	0	20.333	0	0.147	7.81	9.9

For the development of experimental data Table 3.2 refers only to second membrane type) it is necessary to obtain, for each membrane, relationships for the dependence of the permeate flow rate and water separation coefficient upon the process factors values. In this sense, we use the fact that for each membrane, the experimental data was organized according to an experimental plan 2^n (n =3 in this case: permeation temperature (t), pressure in pervaporation chamber (p) and respectively ethanol concentration in the processed mixture (c_{Etoh})).

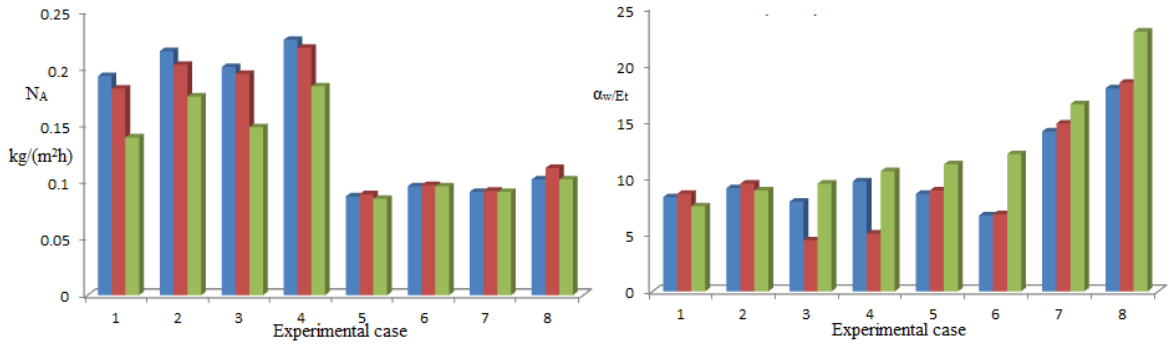

Figure 3.10 State of permeation flow rate and water separation factor for PVA-BC membrane

(blue: membrane 1 PVA/BC = 2, red: membrane 2 PVA/BC = 1, green: membrane 3 PVA/BC = 0.66; experimental case 1, 2, 3, 4, 5, 6, 7, 8 as in Table 3.2)

For the purpose of experimental data development, the following two step procedure was used. Firstly, use the regression analysis with a 2^3 experimental plan in order [83] to obtain the values of the coefficients from dependences $N_A = f(x_1,x_2,x_3)$ and $\alpha_{w/Et} = g(x_1,x_2,x_3)$, these coefficients are shown in equations (3.3) and (3.4). The values for dimensionless temperature

(x_1), dimensionless permeation pressure (x_2) and dimensionless ethanol concentration in the mixture (x_3) are given in equations (3.5) ÷ (3.7).

Secondly, use the obtained values of the above-mentioned coefficients to establish its dependence on the BC membrane content.

$$N_A(x_1, x_2, x_3) = \beta_0 + \beta_1 x_1 + \beta_2 x_2 + \beta_3 x_3 + \beta_{12} x_1 x_2 + \beta_{13} x_1 x_3 + \beta_{23} x_2 x_3 + \beta_{123} x_1 x_2 x_3 \quad (3.3)$$

$$\alpha_{w/Et}(x_1, x_2, x_3) = \alpha_0 + \alpha_1 x_1 + \alpha_2 x_2 + \alpha_3 x_3 + \alpha_{12} x_1 x_2 + \alpha_{13} x_1 x_3 + \alpha_{23} x_2 x_3 + \alpha_{123} x_1 x_2 x_3 \quad (3.4)$$

$$x_1 = \frac{t - t_c}{\Delta t},\ t_c = 50^0 C,\ \Delta t = 10^0 C \quad (3.5)$$

$$x_2 = \frac{p - p_c}{\Delta p},\ p_c = 25.3\ kPa,\ \Delta p = 6.7\ kPa \quad (3.6)$$

$$x_3 = \frac{c_{Etoh} - c_{Etoh\,c}}{\Delta c_{Etoh}},\ c_{Etoh\,c} = 48\ \%\ w,\ \Delta c_{Etoh} = 24\ \%\ w \quad (3.7)$$

The results of the tested membranes contain analytic expressions for N_A =f (x_1,x_2,x_3) and $\alpha_{w/Et}$ = g (x_1,x_2,x_3). The analysis of the obtained relations (three for N_A =f (x_1,x_2,x_3) and three for $\alpha_{w/Et}$ = g (x_1,x_2,x_3)) offers interesting observations.

Table 3.3 Data and results of regression analysis with 2^3 experimental plan for ethanol-water pervaporation with first PVA-BC membrane (PVA/BC=2)

1	Experimental data Matrix (Data) and reproducibility matrix for N_A (Repro1) and $\alpha_{w/Et}$ (Repro2)	Data := $\begin{pmatrix} 1 & -1 & -1 & -1 & 0.193 & 8.3 \\ 2 & 1 & -1 & -1 & 0.215 & 9.1 \\ 3 & -1 & 1 & -1 & 0.201 & 7.9 \\ 4 & 1 & 1 & -1 & 0.225 & 9.7 \\ 5 & -1 & -1 & 1 & 0.087 & 8.6 \\ 6 & 1 & -1 & 1 & 0.096 & 6.8 \\ 7 & -1 & 1 & 1 & 0.091 & 14.1 \\ 8 & 1 & 1 & 1 & 0.102 & 17.9 \end{pmatrix}$ Repro1 := $\begin{pmatrix} 1 & 0 & 0 & 0 & 0.151 \\ 2 & 0 & 0 & 0 & 0.153 \\ 3 & 0 & 0 & 0 & 0.158 \end{pmatrix}$ Repro2 := $\begin{pmatrix} 1 & 0 & 0 & 0 & 10.9 \\ 2 & 0 & 0 & 0 & 10.4 \\ 3 & 0 & 0 & 0 & 9.9 \end{pmatrix}$
2	Significant coefficients in N_A and N_A final expression	$\beta_0 = 0.151$, $\beta_1 = 0.00825$, $\beta_3 = -0.057$ $N_A(x_1,x_2,x_3) = 0.151 + 0.00825x_1 - 0.057x_3$
3	Significant coefficients in $\alpha_{w/Et}$ and $\alpha_{w/Et}$ final expression	$\alpha_0 = 10.3$, $\alpha_2 = 2.1$, $\alpha_3 = 1.55$, $\alpha_{12} = 0.825$, $\alpha_{23} = 2.05$ $\alpha_{w/Et}(x_1,x_2,x_3) = 10.3 + 2.1x_2 + 1.55x_3 + 0.825x_1x_2 + 2.05x_2x_3$
4	Parity representations for N_A and $\alpha_{w/Et}$	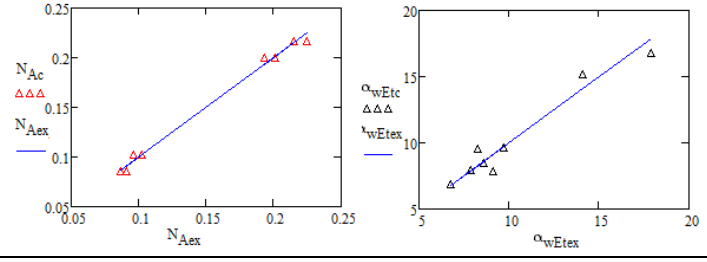

Table 3.4 Data and results of regression analysis with 2^3 experimental plan for ethanol-water pervaporation with second PVA-BC membrane (PVA/BC=1)

1	Experimental data Matrix (Data) and reproducibility matrix for N_A (Repro1) and $\alpha_{w/et}$ (Repro2)	$Data := \begin{pmatrix} 1 & -1 & -1 & -1 & 0.182 & 8.6 \\ 2 & 1 & -1 & -1 & 0.203 & 9.5 \\ 3 & -1 & 1 & -1 & 0.195 & 4.5 \\ 4 & 1 & 1 & -1 & 0.218 & 5.1 \\ 5 & -1 & -1 & 1 & 0.089 & 8.9 \\ 6 & 1 & -1 & 1 & 0.097 & 6.8 \\ 7 & -1 & 1 & 1 & 0.092 & 14.8 \\ 8 & 1 & 1 & 1 & 0.112 & 18.42 \end{pmatrix}$ $Repro1 := \begin{pmatrix} 1 & 0 & 0 & 0 & 0.151 \\ 2 & 0 & 0 & 0 & 0.148 \\ 3 & 0 & 0 & 0 & 0.147 \end{pmatrix}$ $Repro2 := \begin{pmatrix} 1 & 0 & 0 & 0 & 9.2 \\ 2 & 0 & 0 & 0 & 9.6 \\ 3 & 0 & 0 & 0 & 9.9 \end{pmatrix}$
2	Significant coefficients in N_A and N_A final expression	$\beta_0 = 0.149,\ \beta_1 = 0.009, \beta_2 = 0.0057, \beta_3 = -0.051$ $N_A(x_1,x_2,x_3) = 0.149 + 0.009x_1 + 0.0057x_2 - 0.051x_3$
3	Significant coefficients in $\alpha_{w/Et}$ and $\alpha_{w/Et}$ final expression	$\alpha_0 = 9.578,\ \alpha_2 = 1.127, \alpha_3 = 2.652, \alpha_{12} = 0.678, \alpha_{23} = 3.25, \alpha_{123} = 0.75$ $\alpha_{w/Et}(x_1,x_2,x_3) = 9.58 + 1.12x_2 + 2.65x_3 + 0.68x_1x_2 + 3.25x_2x_3 + 0.75x_1x_2x_3$
4	Parity representations for N_A and $\alpha_{w/Et}$	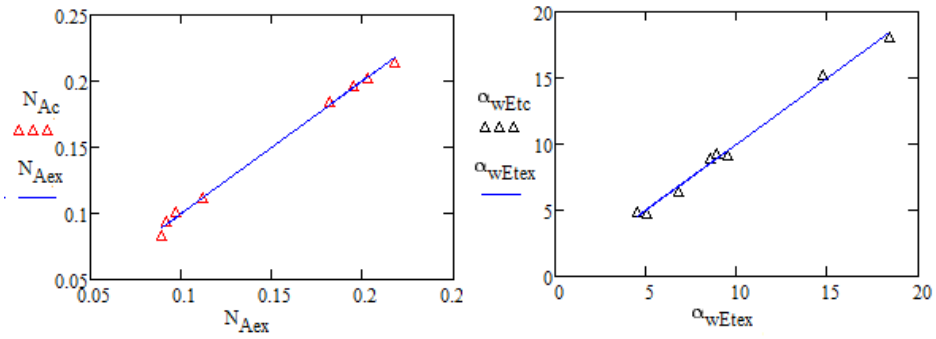

Table 3.5 Data and results of regression analysis with 2^3 experimental plan for ethanol-water pervaporation with third PVA-BC membrane (PVA/BC=0.66)

1	Experimental data Matrix (Data) and reproducibility matrix for N_A (Repro1) and $\alpha_{w/et}$ (Repro2)	$Data := \begin{pmatrix} 1 & -1 & -1 & -1 & 0.139 & 7.5 \\ 2 & 1 & -1 & -1 & 0.175 & 8.9 \\ 3 & -1 & 1 & -1 & 0.148 & 9.5 \\ 4 & 1 & 1 & -1 & 0.184 & 10.6 \\ 5 & -1 & -1 & 1 & 0.085 & 11.2 \\ 6 & 1 & -1 & 1 & 0.096 & 12.1 \\ 7 & -1 & 1 & 1 & 0.091 & 16.5 \\ 8 & 1 & 1 & 1 & 0.102 & 22.9 \end{pmatrix}$ $Repro1 := \begin{pmatrix} 1 & 0 & 0 & 0 & 0.124 \\ 2 & 0 & 0 & 0 & 0.127 \\ 3 & 0 & 0 & 0 & 0.131 \end{pmatrix}$ $Repro2 := \begin{pmatrix} 1 & 0 & 0 & 0 & 11.9 \\ 2 & 0 & 0 & 0 & 12.5 \\ 3 & 0 & 0 & 0 & 12.9 \end{pmatrix}$
2	Significant coefficients in N_A and N_A final expression	$\beta_0 = 0.127,\ \beta_1 = 0.012, \beta_3 = -0.034, \beta_{13} = -0.0062$ $N_A(x_1,x_2,x_3) = 0.127 + 0.012x_1 - 0.034x_3 - 0.0062x_1x_3$
3	Significant coefficients in $\alpha_{w/Et}$ and $\alpha_{w/Et}$ final expression	$\alpha_0 = 12.4,\ \alpha_1 = 1.225, \alpha_2 = 2.475\ \alpha_3 = 3.275, \alpha_{23} = 1.55$ $\alpha_{w/Et}(x_1,x_2,x_3) = 12.4 + 1.225x1 + 2.475x_2 + 3.275x_3 + 1.55x_2x_3$

4	Parity representations for N_A and $\alpha_{w/Et}$	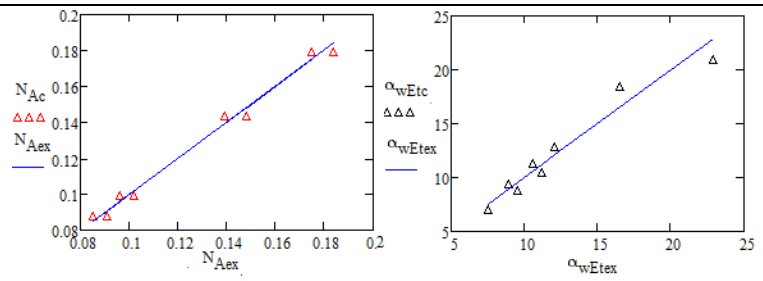

Table 3.6 Unification of $N_A(x_1,x_2,x_3)$ expressions for membranes taking into account the BC content in the membrane

N.C	Parameter	First membrane	Second membrane	Third membrane	Unification relationship
1	BC content in dry membrane %w	2.4	4.8	6.2	-
2	Dimensionless BC content x_4	-1	0	1	-
3	Coefficient β_0	0.151	0.149	0.127	$\beta_0 = 0.149 - 0.012x_4 - 0.034x_4^2$
4	Coefficient β_1	0.00825	0.009	0.012	$\beta_1 = 0.009 + 0.056x_4 + 0.055x_4^2$
5	Coefficient β_2	0	0.00575	0	$\beta_2 = 0$
6	Coefficient β_3	-0.057	-0.051	-0.034	$\beta_3 = -0.051 + 0.268x_4 - 0.251x_4^2$
7	Coefficient β_{13}	0	0	0.00625	$\beta_{13} = 0.00625x_4$

Tabel 3.7 Unification of $\alpha_{w/Et}(x_1,x_2,x_3)$ expressions for membranes taking into account the BC content in the membrane

NC	Parameter	First membrane	Second membrane	Third membrane	Unification relationship
1	BC content in dry membrane %w	2.4	4.8	6.2	-
2	Dimensionless BC content x_4	-1	0	1	-
3	Coefficient β_0	10.3	9.58	12.4	$\beta_0 = 9.58 + 1.05x_4 + 1.77x_4^2$
4	Coefficient β_1	0	0	1.225	$\beta_1 = 0.613x_4 + 0.613x_4^2$
5	Coefficient β_2	2.1	1.27	2.475	$\beta_2 = 1.127 + 0.188x_4 + 1.161x_4^2$
6	Coefficient β_3	1.55	2.65	3.275	$\beta_3 = 2.65 + 0.862x_4 - 0.238x_4^2$
7	Coefficient β_{12}	0.825	0.68	0.05	$\beta_{12} = 0.68 - 0.388x_4 - 0.243x_4^2$
8	Coefficient β_{23}	2.05	3.25	1.55	$\beta_{23} = 0.68 - 0.388x_4 - 0.243x_4^2$
9	Coefficient β_{123}	0	0.75	0	$\beta_{123} = 0.75 - 0.75x_4^2$

In Tables 3.6 and 3.7 can be seen the unification expressions for permeate flux and for water membrane selectivity. In the above-mentioned tables we use, for the BC content in the membrane, the dimensionless form equations (3.8), because the first three process factors are considered with dimensionless expressions.

$$x_4 = \frac{c_{BC} - c_{BC\,c}}{\Delta c_{BC}}\,,\; c_{BC\,c} = 4.8\ \%w\,,\; \Delta c_{BC} = 2.4\ \%w \tag{3.8}$$

With data from Tables 3.6 and 3.7 we can write the unique expressions for permeate flux and water separation factor, which characterize the pervaporation of the ethanol-water system through our PVA-BC membranes. This is expressed in equations (3.9) and (3.10).

$$N_A(x_1, x_2, x_3, x_4) = (0.149 - 0.012x_4 - 0.034x_4^2) + (0.009 + 0.056x_4 + 0.055x_4^2)x_1 + (-0.051 + 0.268x_4 - 0.251x_4^2)x_3 + 0.00625x_4x_1x_3 \tag{3.9}$$

$$\alpha_{\frac{w}{Et}}(x_1, x_2, x_3, x_4) = (9.58 + 1.05x_4 + 1.77x_4^2) + (0.613x_4 + 0.613x_4^2)x_1 + (1.127 + 0.188x_4 + 1.161x_4^2)x_2 + (2.65 + 0.862x_4 - 0.238x_4^2)x_3 + (0.68 - 0.388x_4 - 0.243x_4^2)x_1x_2 + (3.25 - 0.25x_4 - 1.45x_4^2)x_2x_3 + (0.75 - 0.75x_4^2)x_1x_2x_3 \tag{3.10}$$

The length of the final relationships seems complex, but it is normal because it is known that in multi-factor processes, we have ample expressions for the dependence between the response variables and the state of the factors. It is important to note that these two relationships allow the design and simulation of some pervaporation units, equipped with these types of membranes.

3.3 Modelling of pervaporation coupled with fermentation of glucose to ethanol

Pervaporation is one of the most promising approaches to the recovery of alcohols or other solvents (EBA biosynthesis [8,17]) from liquid fermentation culture media. It is simple, non-toxic with regard to the bacterial system that controls the fermentation process, and consumes less energy than classical distillation [18].

3.4.1.2 Modelling the ethanol fermentation reactor

Regarding the exploitation of an ethanol fermentation bioreactor coupled with pervaporation, the present paper proposes the following procedure:

1) start the reactor and setting it in batch operation mode;

2) after an acceptable time period switch the reactor to fed batch operation by feeding it with concentrated substrate;

3) start the pervaporation device in order to control the inhibition of the bacterial cell's activity;

4) stop feeding and return to batch operation with pervaporation;

5) cast off the product as duration or substrate conversion requires it.

3.4.1.3 Fermentation kinetics

Monod equation, equation (3.13), is usually used to correlate the cellular growth rate (v_{RX})with the concentration of the limiting substrate (c_S) in the fermentation processes.

$$v_{RX} = \mu_{max} \frac{c_S}{K_S + c_S} c_X \tag{3.13}$$

Consequently, the Monod model has been completed [44, 45] in order to take into account the influence of all inhibiting factors on the Saccharomyces Cerevisiae cellular growth rate. This is expressed in equation (3.14). Here μ_{max} is the maximum specific growth rate (h^{-1}), K_s the substrate saturation constant (kg/m^3), K_i the substrate inhibition parameter (m^3/kg), C_{Xmax} the cell concentration where growth ceases (kg/m^3), C_{Emax} the ethanol concentration where the cell growth ceases (kg/m^3), K_d the constant of cellular death rate (h^{-1}) and m and n are empirical parameters.

The rate of ethanol formation is dependent on the cellular growth rate. For writing the expression of ethanol formation rate, consider the following observation: When the cells or some constituent of cells that is proportional to cell mass is the product, the rate of product formation directly relates to the rate of growth.

Considering this observation, the ethanol production rate is expressed as shown in equation (3.15), where Y_{EX} (kg/kg) is the product yield based on cell growth and β_E (kg/kg) is a parameter associated with ethanol maintenance by cells. The substrate consumption rate, v_{RS}, equation (3.16), depends on Y_X (kg/kg), the limit cellular yield, and β_S (kg/kg) which is a maintenance parameter similar to β_E.

$$v_{RX} = \mu_{max} \frac{c_S}{K_S + c_S} c_X \left(exp(K_i c_S)\right) \left(1 - \frac{c_X}{c_{Xmax}}\right)^m \left(1 - \frac{c_E}{c_{Emax}}\right)^n - K_d c_X \tag{3.14}$$

$$v_{RE} = Y_{EX} v_{RX} + \beta_E c_X \tag{3.15}$$

$$v_{RS} = \frac{v_{RX}}{Y_X} + \beta_S c_X \tag{3.16}$$

Table 3.10 Characteristic values of parameters characterizing glucose fermentation with a Saccharomyces Cerevisiae bacterial system for t ∈ (20°C- 40°C) and C_S ∈ (50 g/L-250 g/L)

1	$\mu_{\max} = 0.26\left(\frac{t}{20}\right) - 0.075$
2	$K_S = 4.23$, $K_i = 0.002$, $\beta_E = 0.095$, $\beta_S = 0.19$, $m = 1$, $n = 1.5$
3	$c_{X\max} = 269 - 120\left(\frac{t}{20}\right)$
4	$c_{E\max} = 260 - 106\left(\frac{t}{20}\right)$
5	$Y_{EX} = 10.6\left(\frac{t}{20}\right) - 10.25$
6	$Y_X = 0.19 - 0.08\left(\frac{t}{20}\right)$
7	$K_d = 0.54 - 0.12\left(\frac{t}{20}\right)$

3.4.1.4 Process schema and the bioreactor model

Figure 3.12 shows the schema of the coupled process. The pervaporation device is protected from clogging with cellular material by mounting an ultrafiltration device between the bioreactor and the pervaporation device. The bioreactor volume (V), substrate (sugar) concentration (C_S), ethanol concentration (C_E), viable Sacharomyces cerevisiae cell concentration (C_X), dead Sacharomyces cerevisiae cells concentration (C_{Xd}) and carbon dioxide concentration (C_{CO2}) are time variables identified from Figure 3.12. The dynamics of these variables are expressed by total and mass balances of species applied to the bioreactor (equations (3.17)÷(3.22)) which also represent the core of the mathematical model of the coupled process. Other variables which appear in Figure 3.12 are F (m^3/h) - the bioreactor feed rate, F_u (m^3/h) - the bioreactor product rate which will become the feed for the ultrafiltration unit, C_X, C_{Xu} (kg/m^3) – the concentration of active cells in the fermentation medium and those exiting the ultrafiltration unit, C_{Xd}, C_{Xdu} (kg/m^3) – the concentration of dead cells in the fermentation medium and those exiting the ultrafiltration unit, C_S, C_{Sp}, C_{SF} (kg/m^3) – sugar substrate concentration in the fermentation medium, product stream for the pervaporation unit and bioreactor feed, C_E, C_{Ep} (kg/m^3) – ethanol concentration in the fermentation medium and in the retentate stream of the pervaporation unit, N_{tu} ($kg/m^2 \times h$) – total ultrafiltration flux, N_{tp} ($kg/m^2 \times h$) – total pervaporation flux, ρ_{pu} (kg/m^3) – density of ultrafiltration permeate.

$$\frac{dV}{d\tau} = F - \left(\frac{N_{tp}A_p}{\rho_{pu}}\right) \tag{3.17}$$

$$\frac{d(Vc_{Xd})}{d\tau} = VK_d c_X - F_u c_{Xd} + (F_u - \frac{N_{tu}A_u}{\rho_{pu}})c_{Xdu} \tag{3.18}$$

$$\frac{d(Vc_X)}{d\tau} = V(\nu_{RX} - K_d c_X) - F_u c_X + \left(\frac{F_u - N_{tu}A_u}{\rho_{pu}}\right) c_{Xu} \quad (3.19)$$

$$\frac{d(Vc_S)}{d\tau} = -V\nu_{RS} + Fc_{SF} - \frac{N_{tu}A_u c_S}{\rho_{pu}} + \left(\frac{N_{tu}A_u}{\rho_{pu}} - \frac{N_{tp}A_p}{\rho_{pu}}\right) c_{Sp} \quad (3.20)$$

$$\frac{d(Vc_E)}{d\tau} = V\nu_{RE} - \frac{N_{tu}A_u c_E}{\rho_{pu}} + \left(\frac{N_{tu}A_u}{\rho_{pu}} - \frac{N_{tp}A_p}{\rho_{pu}}\right) c_{Ep} \quad (3.21)$$

$$\frac{d(m_{CO2})}{d\tau} = \left[V\nu_{RE} - \frac{N_{tu}A_u c_E}{\rho_{pu}} + \left(\frac{N_{tu}A_u}{\rho_{pu}} - \frac{N_{tp}A_p}{\rho_{pu}}\right) c_{Ep}\right]\left(\frac{M_{CO2}}{M_E}\right) \quad (3.22)$$

The separation factor is a function of glucose concentration, ethanol concentration and

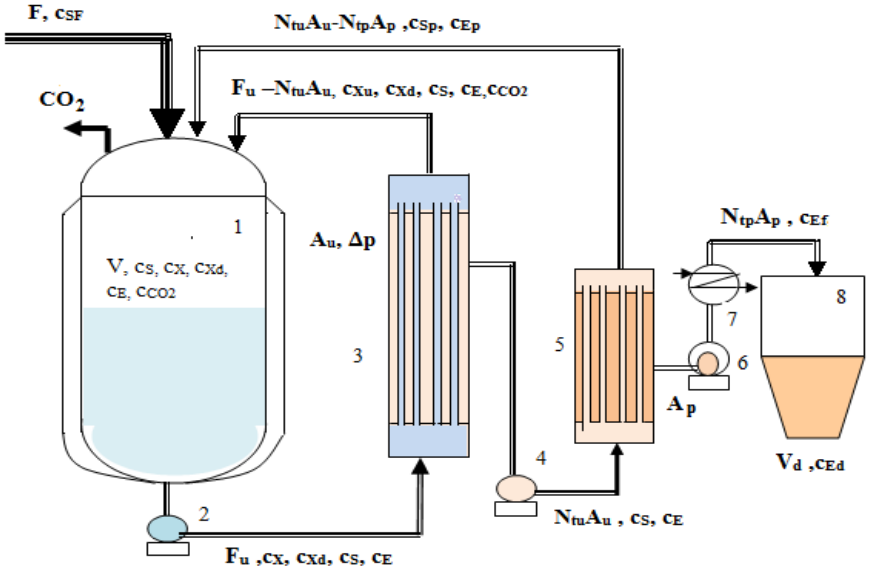

Figure 3.12 Schema of the ethanol fermentation coupled with ultrafiltration and pervaporation (1- fermentation bioreactor, 2- ultrafiltration pump, 3- ultrafiltration device, 4- pump for pervaporation, 5- pervaporation device, 6 – vacuum pump, 7 – cooler, 8 – collecting tank)

temperature. If this is evaluated, then C_{Ef}, equation (3.23), can be computed which also leads to the computation of C_{Ep}, equation (3.24). Equations (3.25), (3.26) and (3.27) are a consequence of the species balance. It is observed that C_{Sp}, C_{Xu} and C_{Xud} are the link between the individual models of the three units used. In addition to these equations, the total flux during ultrafiltration and pervaporation must be expressed.

$$c_{Ef} = \frac{\alpha(c_E)c_E\frac{M_{rp}\rho_{up}}{M_{up}\rho_{rp}}}{\left[1+(\alpha(c_E)-1)\frac{c_E M_{rp}}{\rho_{rp} M_E}\right]} \quad (3.23)$$

$$c_{Ep} = \frac{N_{tu}A_u c_E - N_{tp}A_p c_{Ef}}{N_{tu}} \quad (3.24)$$

$$c_{Sp} = \frac{N_{tu}A_u c_S}{N_{tu}A_u - N_{tp}A_p} \quad (3.25)$$

$$c_{Xu} = \frac{F_u c_X}{F_u - \frac{N_{tu}A_u}{\rho_{pu}}} \quad (3.26)$$

$$c_{Xud} = \frac{F_u c_{Xd}}{F_u - \frac{N_{tu}A_u}{\rho_{pu}}} \quad (3.27)$$

3.4.1.5 Total flux of the ultrafiltration device

Some assumptions regarding the ultrafiltration device were made:

(i) the evolution of ethanol biosynthesis was neglected due to the short residence time of the ultrafiltration retentate;
(ii) the ultrafiltration permeate did not contain any cellular material;
(iii) the solute species concentration was the same in the ultrafiltration retentate and permeate, i.e., C_S and C_E.

Ultrafiltration permeate flux, N_{tu} (kg/(m^2×h), is an important operating parameter characterizing the working capacity of the device.

The series resistance model, which considers this fouling effect due to a gel layer on the membrane surface, is expressed in equation (3.28). Here η (kg/(m×s)) is the permeate viscosity, R_0 (m^{-1}) the initial membrane resistance, r_g (kg/(m^3·s)) the gel layer's specific resistance, Δp (N/m^2) the transmembrane pressure, C_X (kg/m^3) the biomass concentration in the bioreactor, C_{Xg} (kg/m^3) the biomass concentration in the gel layer and τ is the time.

$$N_{tu} = 3{,}55\left(\frac{1}{(\eta R_0)^2 + 3600\frac{2r_g \Delta p c_X}{c_{Xg}}\tau}\right)^{0.5} \Delta p \quad (3.28)$$

3.4.1.6 Model of the coupled process

Equations (3.14) ÷ (3.28) represent the general mathematical model of a fermentation process coupled with external ultrafiltration and pervaporation. Two equations must also be added namely the total balance and the ethanol balance for the pervaporation collecting tank. These are the differential equations (3.29) and (3.30).

$$\frac{dV_d}{d\tau} = \frac{N_{tp}A_p}{\rho_p} \quad (3.29)$$

$$\frac{dc_{Ed}}{d\tau} = \frac{N_{tp}A_p}{\rho_p V_d}\left(c_{Ef} - c_{Ed}\right) \quad (3.30)$$

The center of the mathematical model is based on 8 differential equations, (3.17) ÷ (3.22), (3.29) and (3.30), which determine the dynamics of variables V, C_X, C_{Xd}, C_S, C_E, m_{CO2}, V_d, C_{Ed}.

Table 3.11 Conditions in BF, BFPV and FBFPV

	Process factors	BF	BFPV	FBFPV
1	Initial reactor volume (m^3)	50	50	20
2	Initial sugar concentration (kg/m^3)	150	150	150
3	Initial active cells concentration (kg/m^3)	1.5	1.5	1.5
4	Initial dead cells concentration (kg/m^3)	0.15	0.15	0.15
5	Initial volume of pervaporation collector (m^3)	-	0.01	0.01
6	Initial ethanol concentration in collector (kg/m^3)	-	0.1	0.1
7	Simulation time (h)	100	100	100
8	Surface of ultrafiltration device (m^2)		470/300	470/300
9	Surface of pervaporation device (m^2)		340/170	340/170
10	Pervaporation start time of (h)	-	10	10
11	Fed batch start time (h)	-	-	5
12	Fed batch stop time (h)	-	-	45
13	Feed flow rate in fed batch (m^3/h)	-	-	1.2
14	Sugar concentration in reactor feeding (kg/m^3)	-	-	250
15	Ultrafiltration feed flow rate (m^3/h)	-	20	20
16	Net ultrafiltration pressure difference (bar)	-	1	1
17	Pervaporation permeate pressure (mbar)		70	70
18	Temperature in fermentation bioreactor (^0C)	30	30	30
19	Temperature in pervaporation device (^0C)	60	60	60

3.4.2 Results and discussions

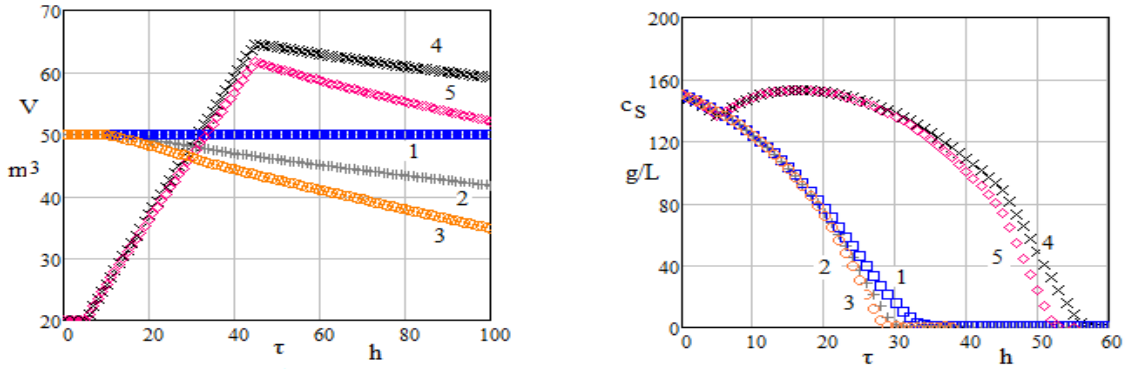

Figure 3.13 Fermentation dynamics respect to active bioreactor volume (V) and sugar concentration (c_S) in the broth (1- BF , 2-BFPV (A_u=340 m^2, A_p=170 m^2, F_u = 20 m^3/h), 3-BFPV (A_u=470 m^2, A_p=340 m^2, F_u = 20 m^3/h),4-FBFPV (A_u=340 m^2, A_p=170 m^2, F_u = 20 m^3/h), 5- FBFPV (A_u=470 m^2, A_p=340 m^2, F_u = 20 m^3/h)

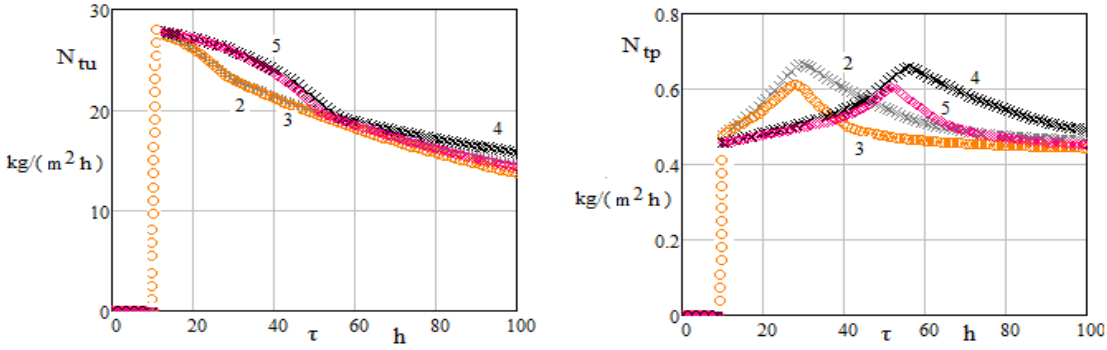

Figure 3.17 Fermentation dynamics respect to permeate flux for ultrafiltration (N_{tu}) and respectively pervaporation (N_{tp}) devices (2 - BFPV (A_u= 340 m^2, A_p= 170 m^2, F_u= 20 m^3/h), 3 - BFPV (A_u= 470 m^2, A_p= 340 m^2, F_u= 20 m^3/h), 4 - FBFPV (A_u= 340 m^2, A_p= 170 m^2, F_u= 20 m^3/h), 5 - FBFPV (A_u= 470 m^2, A_p= 340 m^2, F_u= 20 m^3/h)

Table 1.12 Main results for BF, BFPV and FBFPV fermentation modes

	Operating mode Process major results	BF	BFPV 300/170	BFPV 470/340	FBFPV 300/170	FBFPV 470/340
1	Initial volume of the broth (m^3)	50	50	20	20	20
2	Initial sugar concentration in reactor (g/l)	150	150	150	150	150
3	Sugar concentration in the reactor feed (g/l)	-	-	-	250	250
4	Final ethanol concentration in reactor (g/l)	70.86	9.13	5.41	14.39	5.69
5	Final sugar in reactor (g/l)	0.623	0.28	0.092	0.12	0.07
6	Ethanol in pervaporation collector (g/l)	-	383	231	773.2	423
7	Sugar processed mass (kg)	$7.469\cdot10^3$	$7.488\cdot10^3$	$7.503\cdot10^3$	$14.99\cdot10^3$	$15.1\cdot10^3$
8	Ethanol resulted mass (kg)	$3.583\cdot10^3$	$3.514\cdot10^3$	$3.656\cdot10^3$	$7.07\cdot10^3$	$7.08\cdot10^3$
9	Carbon dioxide resulted mass (kg)	$3.484\cdot10^3$	$3.467\cdot10^3$	$3.499\cdot10^3$	$6.86\cdot10^3$	$6.89\cdot10^3$
10	Active cells mass at finish (kg)	257.9	269.3	274.1	329.7	432.7
11	Died cells mass at finish (kg)	264.3	272.6	270.6	268.6	289.6
12	Sugar conversion to ethanol	0.461	0.459	0.465	0.461	0.461
13	Water mass to be evaporated for one kilo of absolute ethanol (kg/kg)	9.98	1.41	3.11	0.276	1.213

It is clearly demonstrated that the greatest advantage of coupled fermentation is to control the inhibition of the fermentation process and to obtain a pervaporation product with a high concentration of ethanol. The biggest disadvantage of BFPV and FBFPV fermentation modes is the high surface values for coupled ultrafiltration and pervaporation units.

Selective bibliographic references

[8]. Sandu Ohreac B., Dobre T., Pârvulescu O. C., Danciu D. T., Integration of ABE solvents batch biosynthesis with their recovery by gas stripping., Rev. Chim. (Bucharest), 65, 5, 582-592, 2014
[17]. Dong Z., Gongping L., Sainan L., Zhengkun L., Wanqin J., High performance ceramic hollow fiber supported PDMS composite pervaporation membrane for bio-butanol recovery, Journal of Membrane Science 450, 38–47, 2014.
[18]. Lee H.J., Cho E.J., Kim Y.G., Choi I.S., Bae H.J., Pervaporative separation of bioethanol using a polydimethylsiloxane/polyetherimide composite hollow fiber membrane, Bioresour. Technol. 109, 110–115,2012
[44]. Rivera C. E., Costa C. A., Atala I.P. D., Maugeri F., Maciel R. W. M., Maciel R. F., Evaluation of optimization techniques for parameter estimation: Application to ethanol fermentation considering the effect of temperature, Proces Biochemistry, 41,1682-1687, 2006
[45]. Rivera C. E., Yamakawaa K. C., Garcia H. M., Geraldoa C. V., Rossella E.V. C., Maciel F., Bonomia A., A Procedure for Estimation of Fermentation Kinetic Parameters in Fed-Batch Bioethanol Production Process with Cell Recycle, Chemical Engineering Transactions, 32, 1369-1374, 2013

CHAPTER 4
Modeling of ABE fermentation control schemes for control of product inhibition effects

4.4.4 Semi-continuous ABE synthesis with gas stripping

Fed-batch reactors are widely used in industrial applications because they combine both the advantages of discontinuous (batch) and continuous-functioning processes.

The physical model used to describe EBA biosynthesis in a gas stripping solvent and stirring bioreactor is schematically represented in Figure 4.2. In this paper, a sequential operation of the bioreactor was selected, i.e. batch mode in the first sequence, fed-batch mode in the second sequence that begins at the time of switching τ_{sw}, fed-batch with the gas stripping of the species in the third sequence that begins at the start time of the stripping τ_{str}, respectively and depending on the case, there is batch with gas stripping until the operation of the batch ends. This modus operandi, absent in most of the work on the integration of EBA fermentation with gas stripping, is new in the analysis of the process. His supportive hypotheses are that: i) you do not have to start stripping in the early stages of fermentation because here we are in the acidogenesis phase and stripping will not take effect; (ii) the transition from batch to fed-batch of reactor operation must be made when it has started to work with intensity; iii) it would be good for the fed-batch mode with stripping to move into the final phase of the batch with stripping (case not analyzed in this paper).

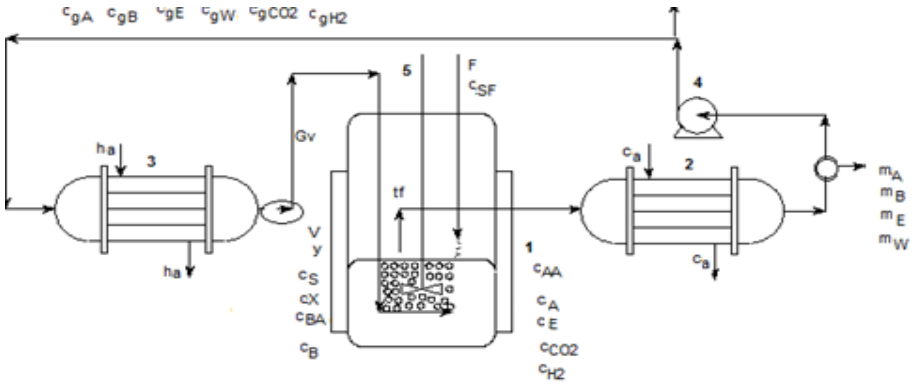

Figure 4.2 Scheme of an EBA process controlled by gas stripping (1-bioreactor, 2-condenser cooler, 3 – gas heater, 4-gas recirculation pump)

Other hypotheses considered for the modeling of the fed-batch reactor with gas stripping are the following:

1. Stripping gas leaves the cooler (2) saturated with species vapour at a concentration which in the liquid phase is c_i, i=A, B, E, W.
2. Carbon dioxide and hydrogen accumulate in the stripping gas at the current levels of current concentration cg_{CO2} and cg_{H2} (i.e. the volume of gas accumulation is sufficiently high in relation to the volume of biosynthesis).
3. The gas-liquid balance of species A, B, E and W in relation to the fermentation medium shall be expressed by the distribution coefficient k_{di}, i=A, B, E, W and by the coefficient of activity of the same species in the liquid medium (μ_i, i=A, B, E, W, CO_2, H_2). Consideration of the ideal behavior of the components mentioned in the liquid phase requires consideration of the unit value for all activity coefficients.
4. The resistance to mass transfer of species A, B, E, CO_2 and H_2 in the fermentation suspension is located in the liquid film surrounding the bubbles forming in fermentation, while for water (W) it is located in the gaseous phase.

Under these conditions, the mass flow rate of the component i vaporized inside the bioreactor, n_{Si}, is expressed by the equation (4.20) in which the c_i (g/L or kg/m^3) is the concentration of compound i in the environment and c_{gi} expresses the concentration of the component i in the stripping gas. Here the volumetric mass transfer coefficient k_{lai} (hr-1) is refers to the liquid film, and μ is the activity coefficient of the species i in the liquid phase. The concentration of the component i in the recirculation gas is expressed by the Antoine relationship (4.21).

$$n_{si} = V k_{lai}\left[\mu_i c_i - k_{di} c_{gi}(t_c)\right] \qquad \text{i=A, B, E, } CO_2, H_2 \qquad (4.20)$$

$$c_{gi} = \frac{m_i}{RT_f \sum_{i=1}^{4} \frac{m_i}{M_i}} 10^{A_i - \frac{B_i}{C_i + t_c}} \qquad \text{i=A, B, E} \qquad (4.21)$$

As is already known the mathematical model, which characterizes the dynamics of the components in the bioreactor with perfect mixing, is based on the general relationship (4.22) of the non-stationary mass balance of the species in the fermentation environment.

$$\frac{D(Vc_i)}{d\tau} = VR_i + Fc_{SF} - n_{si} \qquad \text{i=X,S,A,B,E,AA,BA,CO}_2\text{,H}_2 \tag{4.22}$$

In agreement with the above, taking into consideration simplification hypotheses, including species generation/consumption, the mathematical model characteristic of EBA biosynthesis for a bioreactor working with the stripping of volatile compounds (solvents) contains equations (4.23) – (4.39).

$$\frac{dV}{d\tau} = F(\tau) - \frac{1}{\rho_A}\frac{dm_A}{d\tau} - \frac{1}{\rho_B}\frac{dm_B}{d\tau} - \frac{1}{\rho_E}\frac{dm_E}{d\tau} - \frac{1}{\rho_W}\frac{dm_W}{d\tau} \tag{4.23}$$

$$\frac{dy}{d\tau} = \left[k_l K_l \frac{c_S}{K_l + c_B} - 0.56(y-1) \right] y \tag{4.24}$$

$$\frac{dc_X}{d\tau} = 0.56(y-1)c_x - k_2 c_B c_x - \frac{F}{V}c_X \tag{4.25}$$

$$\frac{dc_S}{d\tau} = -k_3 c_S c_X - k_4 \frac{c_S c_X}{c_S + k_S} - \frac{F}{V}(c_{SF} - c_S) \tag{4.26}$$

$$\frac{dc_{BA}}{d\tau} = k_5 \frac{k_l c_S}{k_l + c_B} c_X - k_6 \frac{c_{BA}}{c_{BA} + k_{BA}} c_X - \frac{F}{V} c_{BA} \tag{4.27}$$

$$\frac{dc_B}{d\tau} = k_7 c_S c_X - 0.8\left(\frac{dc_B}{d\tau} + \frac{F}{V}c_{BA}\right) - \frac{F}{V}c_B - k_{lB}a\left[\mu_B c_B - \frac{k_{dB} m_B}{RT_f \sum_{i-1}^{4} \frac{m_i}{M_i}} 10^{\left(A_B - \frac{B_B}{c_B + t_c}\right)}\right] \tag{4.28}$$

$$\frac{dc_{BA}}{d\tau} = k_8 \frac{c_S}{c_S + k_S}\frac{k_l}{k_l + c_B} c_X - k_9 \frac{c_{AA}}{c_{AA} + k_{AA}} c_X - \frac{F}{V} c_{AA} \tag{4.29}$$

$$\frac{dc_A}{d\tau} = k_{10} \frac{c_S}{c_S + k_S}\, c_X - 0.5\left(\frac{dc_{AA}}{d\tau} + \frac{F}{V}c_{AA}\right) - \frac{F}{V}c_A - k_{lA}a\left(\mu_A c_A - \frac{k_{dA} m_A}{RT_f \sum_{i-1}^{4} \frac{m_i}{M_i}} 10^{\left(A_A - \frac{B_A}{c_A + t_c}\right)}\right) \tag{4.30}$$

$$\frac{dc_E}{d\tau} = k_{11} \frac{c_S}{c_S + k_S}\, c_X - \frac{F}{V}c_E - k_{lE}a\left[\mu_E c_E - \frac{k_{dE} m_E}{RT_f \sum_{i-1}^{4} \frac{m_i}{M_i}} 10^{\left(A_E - \frac{B_E}{c_E + t_c}\right)}\right] \tag{4.31}$$

$$\frac{dc_{CO_2}}{d\tau} = k_{12} \frac{c_S}{c_S + k_S}\, c_X - \frac{F}{V}c_{CO_2} - k_{lCO_2}a\left(\mu_{CO2} c_{CO_2} - k_{dCO_2} c_{gCO_2}\right) \tag{4.32}$$

$$\frac{dc_{H_2}}{d\tau} = k_{13} \frac{c_S}{c_S + k_S}\, c_X + k_{14} c_S c_X - \frac{F}{V}c_{H_2} - k_{lH_2}a\left(\mu_{H2} c_{H_2} - k_{dH_2} c_{gH_2}\right) \tag{4.33}$$

$$\frac{dc_{gCO_2}}{d\tau} = \frac{k_{lCO_2} aV\left(\mu_{Co2} c_{CO_2} - k_{dCO_2} c_{gCO_2}\right)}{V_g} \tag{4.34}$$

$$\frac{dc_{gH_2}}{d\tau} = \frac{k_{lH_2} aV\left(\mu_{H2} c_{H_2} - k_{dH_2} c_{gH_2}\right)}{V_g} \tag{4.35}$$

$$\frac{dm_A}{d\tau} = k_{lA}aV\left[\mu_A c_A - \frac{k_{dA}m_A}{RT_f\sum_{i-1}^{4}\frac{m_i}{M_i}}10^{\left(A_A-\frac{B_A}{C_A+t_c}\right)}\right] \quad (4.36)$$

$$\frac{dm_B}{d\tau} = k_{lB}aV\left[\mu_B c_B - \frac{k_{dB}m_B}{RT_f\sum_{i-1}^{4}\frac{m_i}{M_i}}10^{\left(A_B-\frac{B_B}{C_B+t_c}\right)}\right] \quad (4.37)$$

$$\frac{dm_E}{d\tau} = k_{lE}aV\left[\mu_E c_E - \frac{k_{dE}m_E}{RT_f\sum_{i-1}^{4}\frac{m_i}{M_i}}10^{\left(A_E-\frac{B_E}{C_E+t_c}\right)}\right] \quad (4.38)$$

$$\frac{dm_W}{d\tau} = M_W\frac{k_{gW}aV}{RT_f}[10^{\left(A_W-\frac{B_W}{C_W+t_f}\right)} - (10^{\left(A_W-\frac{B_W}{C_W+t_f}\right)}] \quad (4.39)$$

It is interesting to mention that from a technological point of view the synthesis of EBA is characterized by the function expressing carbon fixation in the form of solvents. For the operation of the fed-batch with solvent stripping, described above, this function will depend, directly or indirectly, on the fed-batch reactor feed flow rate, the substrate concentration of the feed, the time when the fed-batch operations begin and the time when the solvent stripping begins. These variables, listed as an argument in F_{opt} , do not appear as direct variables on the right side of the expression (4.40), expressing the carbon content in EBA fermentation solvents.

$$F_{opt}(F, c_{SF}, \tau_{sw}, \tau_{str}) = \frac{0.622m_A}{V_f} + \frac{0.646m_B}{V_f} + \frac{0.527m_E}{V_f} + 0.646\left(c_B - \frac{V_0 c_{B0}}{V_f}\right) + 0.622\left(c_{Af} - \frac{V_0 c_{A0}}{V_f}\right)c_{Af} + 0.527\left(c_{Ef} - \frac{V_0 c_{E0}}{V_f}\right)c_{Ef} - 0.4c_{Sf} - 0.4806c_{Xf} - 0.44c_{AAf} - 0.4865c_{Bf}) \quad (4.40)$$

In the expression (4.40) subscript f refers to the final state of fermentation, and numerical coefficients show the participation of carbon in solvent molecules.

4.4.5 Examples of simulation of the functioning of EBA synthesis, fed-batch with stripping

The kinetic model of the process containing, as result from the above, 18 differential equations, used numerical integration with the help of MATLAB software to express its dynamics.

Semi-continuous (fed-batch) fermentation with stripping, considered in the representations given below, starts from the fact that at 15, 20 and even 25 hours of the process the gas stripping begins. Table 4.3 specifies some of the conditions for simulating the fermentation conducted as described above. It should be noted that a feed flow rate closely related to the initial volume of the batch fermentation start is kept in this table. The results of a model simulation with a large number of response variables and a large number of manipulable variables (controllable input variables) are quite complex.

Table 4.3 EBA Synthesis Simulation Conditions when operating fed-batch with stripping

Variables	Name of variable	Symbol	Values set	UM
Manipulated	Time of change of operating regime	τ_{sw}	10	h
	Feed flow rate	F	$0.04V_0$	m^3/h
	Glucose concentration in feed flow rate	c_{SF}	100	g/L
Initial fixed	Glucose concentration	c_{S0}	50	g/L
	Biomass concentration	c_{X0}	0,6	g/L
	Butanol concentration	c_{B0}	0,5	g/L
	Acetone concentration	c_{A0}	0,81	g/L
	Ethanol concentration	c_{E0}	0,24	g/L
	Butyric acid concentration	c_{BA0}	4,78	g/L
	Acetic acid concentration	c_{AA0}	3,68	g/L
	CO_2 concentration	c_{C020}	0	g/L
	H_2 concentration	c_{H20}	0	g/L
	Concentration of metabolic activity marker and the initial volume of the start of fermentation	y_0	1,2	-
		V_0	20	m^3

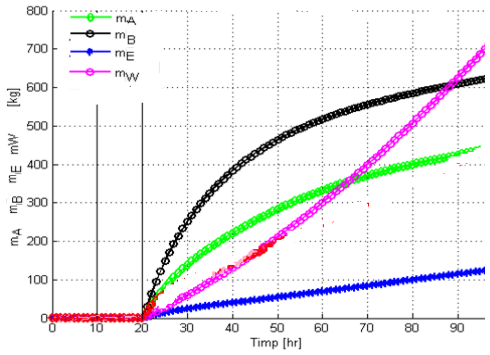

Figure 4.5 Dynamics of the collection of condensed solvents and water (m_A, m_B, m_E, m_W) for the conditions c_{S0} =50 g/L, F =0.04 V_0 m^3/h, t =37ºC, V_0 =20 m^3, c_{SF} =50 g/L, y_0=1,2, τ_{sw} =10 h, τ_{str} =20 h

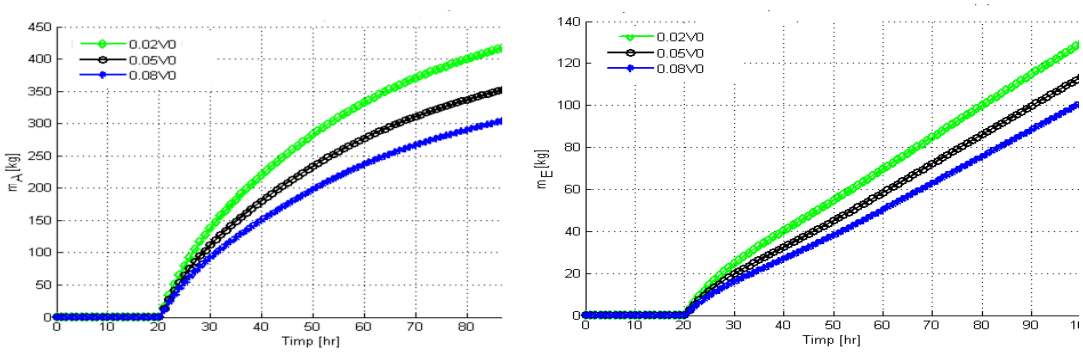

Figure 4.7 Dynamics of the mass of acetone and ethanol at different reactor feed flows rate (green 0,02 V_0, black 0,05 V_0 and blue 0.08 V_0 m^3/h) and operating conditions c_{S0} =50 g/L, t =37ºC, V_0 =20 m^3, c_{SF} =50 g/L, y_0=1.2, τ_{sw} =10 h, τ_{str} =20 h

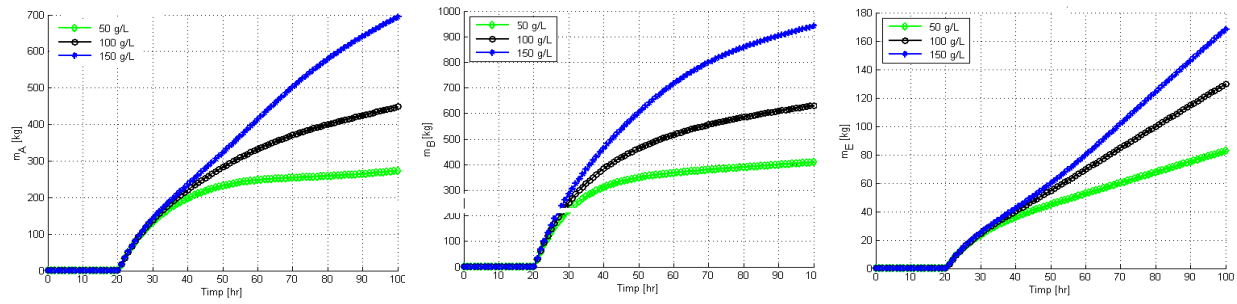

Figure 4.9 Dynamics of the mass of acetone, butanol and ethanol separated in the condenser according to the concentration of the substrate in the reactor feed (50 g/L, 100 g/L and 150 g/L) for the operating conditions c_{S0} =50 g/L, t =37ºC, V_0 =20 m^3, F =0.04 V_0 m^3/h, y_0=1.2, τ_{sw} =10 h, τ_{str} =20h

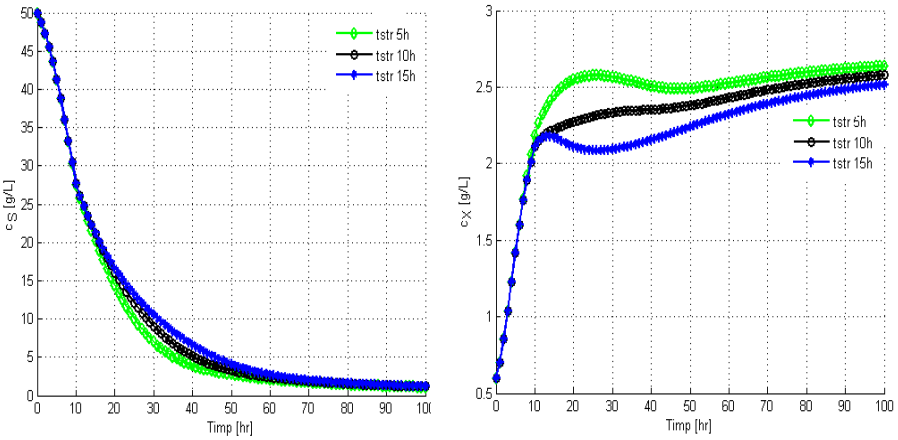

Figure 4.11 Effect of starting gas stripping on the concentration of the substrate (glucose) and cellular mass in the fermenter when operating with c_{S0} =50 g/L, c_{SF} =50 g/L, t =37ºC, V_0 =20 m^3, F =0.04 V_0 m^3/h, y_0=1.2, τ_{sw} =10 h

4.4.6 Formulation of optimization problem

The solution chosen in this paper was to limit the number of factors to those with high sensitivity, to build for them a response area for one or more specific response functions. From the simulations of the proposed operating model we can consider as high sensitivity factors : substrate concentration in reactor feed (c_{SF}), start time of stripping τ_{str}, switching time from batch to fed-batch operation (τ_{sw}) and feed flow rate (F). The first objective function chosen in the formulation of the optimization problem is the mass of carbon fixed in solvents for the reactor volume unit [20]. It is expressed by the relationship (4.41) in which the positive terms, with the coefficients of presence of carbon in the solvent, show the useful fixation (in solvents) of carbon, and the negative terms, with specific numerical coefficients, show the carbon which is not fixed (unreacted) or linked in biomass, in acetic acid and butyric acid respectively.

$$F_{opt}(F, c_{SF}, \tau_{sw}, \tau_{str}) = \frac{0.622 m_A}{V_f} + \frac{0.646 m_B}{V_f} + \frac{0.527 m_E}{V_f} + 0.646\left(c_B - \frac{V_0 c_{B0}}{V_f}\right) + 0.622\left(c_{Af} - \frac{V_0 c_{A0}}{V_f}\right) c_{Af} + 0.527\left(c_{Ef} - \frac{V_0 c_{E0}}{V_f}\right) c_{Ef} - 0.4 c_{Sf} - 0.4806 c_{Xf} - 0.44 c_{AAf} - 0.4865 c_{Bf}) \quad (4.41)$$

Table 4.4 Manipulated variables (high sensitivity process factors) and fixed variables

Variable type	Variable name	Symbol	Value	u.m
Manipulated variables	Substrate concentration in feed	c_{SF}	50, 100, 150	g/L
	Time to start stripping	τ_{str}	10, 30, 50	h
	Time of change from batch	τ_{sw}	5, 15, 25	h
	Feed flow rate	F	$0.03V_0$,$0.06V_0$,$0.09\ V_0$	m^3/h
Variables initially fixed	Glucose concentration	c_{S0}	80	g/L
	Biomass concentration	c_{X0}	0,6	g/L
	Butanol concentration	c_{B0}	0,5	g/L
	Acetone concentration	c_{A0}	0,81	g/L
	Ethanol concentration	c_{E0}	0,24	g/L
	Butyric acid concentration	c_{BA0}	4,8	g/L
	Acetic acid concentration	c_{AA0}	3,7	g/L
	CO_2 concentration	c_{C020}	0	g/L
	H_2 concentration	c_{H20}	0	g/L
	Concentration of metabolic activity marker	y_0	1,2	-
		V_0	20	m^3

Table 4.4 shows the levels of process factors (manipulated variables) and the initial fixed values so that the process model can be simulated. With the help of the second-order orthogonal plane is aimed to obtain an analytical expression for the optimized function, $F_{opt}(F, c_{SF}, \tau_{sw}, \tau_{str})$, respectively for the remaining substrate concentration in the fermentation medium, $c_{Sf}(F, c_{SF}, \tau_{sw}, \tau_{str})$. In the development of data by the orthogonal plane of order 2, the process factors are used in dimensionless form and have general expression through the relationship (4.42). Which has the concrete particularizations (4.43) ÷ (4.46) for the dimensionless feed concentration, x_1, the dimensionless starting time of gas stripping, x_2, the dimensionless shift time from batch operation to fed-batch operation, x_3, and the dimensionless feed flow rate, x_4 respectively.

In the calculation of data processing according to the orthogonal plane of order 2 the derived dimensionless factor , x_j' is used, which is important in the calculation of the coefficients of square influences in the analytical expressions of the response considered in the process. In this case the model's response to the modification of the dimensionless factors x_1 ÷ x_4 is expressed by the state of the function, $F_{opt}(x_1, x_2, x_3, x_4)$ when are modified the factors in the argument, the relationship (4.48), respectively by the state of the minimum substrate

concentration in the environment, $c_{Sf}(x_1, x_2, x_3, x_4)$, when $x_1 \div x_4$ have the combinations of the orthogonal program of order 2, the relationship (4.47).

$$x_j = \frac{z_j - z_{j,C}}{\Delta z_j} = \frac{z_j - \frac{z_{j,max} + z_{j,min}}{2}}{\frac{z_{j,max} - z_{j,min}}{2}}, j = 1 \dots 4 \quad (4.42)$$

$$x_1 = \frac{c_{SF} - c_{SfC}}{\Delta c_{SF}}, c_{SfC} = 100,\ \Delta c_{SF} = 50 \quad (4.43)$$

$$x_2 = \frac{\tau_{str} - \tau_{strc}}{\Delta \tau_{str}}, \tau_{strc} = 30,\ \Delta \tau_{str} = 20 \quad (4.44)$$

$$x_3 = \frac{\tau_{sw} - \tau_{swc}}{\Delta \tau_{sw}}, \tau_{swc} = 15,\ \Delta \tau_{sw} = 10 \quad (4.45)$$

$$x_4 = \frac{F - F_C}{\Delta F},\ F_c = 0.06V_0,\ \Delta F = 0.03V_0 \quad (4.46)$$

$$x_j' = x_j^2 - \frac{\sum_{i=1}^{25} x_{ji}^2}{25} = x_j^2 - \bar{x}_j^2, j = 1 \dots 4 \quad (4.47)$$

$$F_{opt}(x_1, x_2, x_3, x_4) = + \sum_{i=1}^{4} \beta_i x_i + \sum_{i=1}^{4} \sum_{j=i+1}^{4} \beta_{ij} x_i x_j + \sum_{i=1}^{4} \sum_{j=i+1}^{4} \sum_{k=j+1}^{4} \beta_{ijk} x_i x_j x_k + \beta_{1234} x_1 x_2 x_3 x_4 + \sum_{i=1}^{4} \beta_{ii} (x_i^2 - x_{ci}) \quad (4.48)$$

$$c_{Sf}(x_1, x_2, x_3, x_4) = + \sum_{i=1}^{4} \alpha_i x_i + \sum_{i=1}^{4} \sum_{j=i+1}^{4} \alpha_{ij} x_i x_j + \sum_{i=1}^{4} \sum_{j=i+1}^{4} \sum_{k=j+1}^{4} \alpha_{ijk} x_i x_j x_k + \alpha_{1234} x_1 x_2 x_3 x_4 + \sum_{i=1}^{4} \alpha_{ii} (x_i^2 - x_{ci}) \quad (4.49)$$

The working procedure contains the sequences:

1. For the current dimensionless combination of factorial plane factors of order 2, their dimensional values will be established;
2. The dimensional values of the factors, as set out above, are used as input data in the EBA fermentation simulation program with batch→fed-batch→gas stripping operation;
3. The simulation program provides the F_{opt} and c_{SF} values to be brought into the working matrix of the orthogonal plane of order 2;
4. After completing the matrix of the orthogonal plan of order 2 it will be introduced as the input data, in the data development program that provides the coefficients β and α of relations (4.48) and (4.49) respectively.

Table 4.5 Factor combination and response of the process for determining dependencies, $F_{opt}(x_1, x_2, x_3, x_4)$ and $c_{Sf}(x_1, x_2, x_3, x_4)$ with the help of the second-order orthogonal factorial plan

N.c	c_{SF} g/L	x_1	τ_{str} h	x_2	τ_{sw} h	x_3	F m^3/h	x_4	F_{opt} g/L	c_{sf} g/L
1	150	1	50	1	25	1	0.09 V_0	1	16.69	5.31
2	50	-1	10	-1	25	1	0.09V_0	1	5.83	0.85
3	150	1	10	-1	5	-1	0.09V_0	1	13.19	1.5
4	50	-1	50	1	5	-1	0.09V_0	1	6.16	0.69
5	150	1	10	-1	25	1	0.03V_0	-1	14.21	1.79

6	50	-1	50	1	25	1	$0.03V_0$	-1	7.21	2.26
7	150	1	50	1	5	-1	$0.03V_0$	-1	21.29	4.76
8	50	-1	10	-1	5	-1	$0.03V_0$	-1	6.78	0.76
9	150	1	10	-1	25	1	$0.09V_0$	1	13.91	1.51
10	50	-1	50	1	50	1	$0.09V_0$	1	4.92	2.21
11	150	1	50	1	5	-1	$0.09V_0$	1	18.48	4.77
12	50	-1	10	-1	5	-1	$0.09V_0$	1	5.81	0.74
13	150	1	50	1	25	1	$0.03V_0$	-1	19.82	5.31
14	50	-1	10	-1	25	1	$0.03V_0$	-1	6.35	0.85
15	150	1	10	-1	5	-1	$0.03V_0$	-1	15.67	1.51
16	50	-1	50	1	5	-1	$0.03V_0$	-1	7.32	1.87
17	100	0	30	0	15	0	$0.06V_0$	0	9.67	1.52
18	170	1.41	30	0	15	0	$0.06V_0$	0	20.37	2.33
19	30	-1.41	30	0	15	0	$0.06V_0$	0	5.65	0.81
20	100	0	58.2	1.41	15	0	$0.06V_0$	0	9.83	6.45
21	100	0	2	-1.41	15	0	$0.06V_0$	0	7.45	1.14
22	100	0	30	0	29.5	1.41	$0.06V_0$	0	9.86	1.72
23	100	0	30	0	1	-1.41	$0.06V_0$	0	10.31	1.34
24	100	0	30	0	15	0	$0.102V_0$	1.41	8.59	1.53
25	100	0	30	0	15	0	$0.0177V_0$	-1.41	11.55	1.52

Table 4.6 Matrix of the second-order orthogonal factorial program with F_{opt} and c_{Sf} in columns 9 and 10

Data =

	0	1	2	3	4	5	6	7	8
9	10	-1	1	1	1	0.2	0.2	0.2	0.2
10	11	1	1	-1	1	0.2	0.2	0.2	0.2
11	12	-1	-1	-1	1	0.2	0.2	0.2	0.2
12	13	1	1	1	-1	0.2	0.2	0.2	0.2
13	14	-1	-1	1	-1	0.2	0.2	0.2	0.2
14	15	1	-1	-1	-1	0.2	0.2	0.2	0.2
15	16	-1	1	-1	-1	0.2	0.2	0.2	0.2
16	17	0	0	0	0	-0.8	-0.8	-0.8	-0.8
17	18	1.41	0	0	0	1.2	-0.8	-0.8	-0.8
18	19	-1.41	0	0	0	1.2	-0.8	-0.8	-0.8
19	20	0	1.41	0	0	-0.8	1.2	-0.8	-0.8
20	21	0	-1.31	0	0	-0.8	1.2	-0.8	-0.8
21	22	0	0	1.41	0	-0.8	-0.8	1.2	-0.8
22	23	0	0	-1.41	0	-0.8	-0.8	1.2	-0.8
23	24	0	0	0	1.41	-0.8	-0.8	-0.8	1.2
24	25	0	0	0	-1.41	-0.8	-0.8	-0.8	...

Data =

	3	4	5	6	7	8	9	10	11
9	1	1	0.2	0.2	0.2	0.2	4.92	2.21	0.39
10	-1	1	0.2	0.2	0.2	0.2	18.44	4.77	2.02
11	-1	1	0.2	0.2	0.2	0.2	5.81	0.74	1.23
12	1	-1	0.2	0.2	0.2	0.2	19.82	2.31	1.09
13	1	-1	0.2	0.2	0.2	0.2	6.36	0.85	0.29
14	-1	-1	0.2	0.2	0.2	0.2	15.67	1.51	1.89
15	-1	-1	0.2	0.2	0.2	0.2	7.32	1.87	1.35
16	0	0	-0.8	-0.8	-0.8	-0.8	9.67	1.52	1.45
17	0	0	1.2	-0.8	-0.8	-0.8	20.37	2.33	1.81
18	0	0	1.2	-0.8	-0.8	-0.8	6.65	0.81	0.25
19	0	0	-0.8	1.2	-0.8	-0.8	9.83	6.45	1.45
20	0	0	-0.8	1.2	-0.8	-0.8	7.45	1.14	1.22
21	1.41	0	-0.8	-0.8	1.2	-0.8	9.86	1.75	1.22
22	-1.41	0	-0.8	-0.8	1.2	-0.8	10.31	1.34	1.28
23	0	1.41	-0.8	-0.8	-0.8	1.2	8.59	1.53	1.05
24	0	-1.41	-0.8	-0.8	-0.8	1.2	11.55	1.52	...

Table 4.7 Reproducibility estimation matrix for Fopt (left) and cSf

$$\text{Repro} = \begin{pmatrix} 1 & 0 & 0 & 0 & 0 & 11.2 \\ 2 & 0 & 0 & 0 & 0 & 11.536 \\ 3 & 0 & 0 & 0 & 0 & 10.864 \\ 4 & 0 & 0 & 0 & 0 & 10.976 \end{pmatrix} \qquad \text{Repro} = \begin{pmatrix} 1 & 0 & 0 & 0 & 0 & 2.07 \\ 2 & 0 & 0 & 0 & 0 & 2.484 \\ 3 & 0 & 0 & 0 & 0 & 1.822 \\ 4 & 0 & 0 & 0 & 0 & 2.029 \end{pmatrix}$$

Relationships (4.50) and (4.51) express the dependencies for F_{opt} and c_{Sf} on the four process factors (dimensionless substrate concentration to feed (x_1), dimensionless start time of stripping (x_2), dimensionless starting time of batch→fed-batch (x_3) passage and dimensionless flow rate of substrate feed (x_4)).

$$F_{opt}(x_1, x_2, x_3, x_4) = 11.116 + 4.146x_1 + 1.02x_2 - 0.286x_3 - 0.686x_4 + 1.152x_1x_2 - 0.238x_1x_4 - 0.322x_2x_4 - 0.252x_2x_3x_4 + 1.919({x_1}^2 - 0.8) - 0.518({x_2}^2 - 0.8) \quad (4.50)$$

$$c_{Sf}(x_1, x_2, x_3, x_4) = 2.72 + 0.6486x_1 + 0.729x_2 + 0.419x_1x_2 + 0.267x_1x_4 + 0.22x_3x_4 - 0.225x_1x_2x_3 + +0.31x_1x_2x_4 + 0.255x_2x_3x_4 + 0.893({x_2}^2 - 0.8) - 0.232({x_3}^2 - 0.8) - 0.242({x_4}^2 - 0.8) \quad (4.51)$$

Before moving on to an analysis of these relationships, which in them concentrate the essence of the proposed control solution for EBA fermentation, it should be said that the major interest in these solutions is to find, if possible, that combination of factors that maximize F_{opt} and minimize c_{Sf}. This effort consists in solving the systems of equations (4.52) and (4.53), respectively, through which we seek the extreme of the functions, $F_{opt}(x_1, x_2, x_3, x_4)$ and $c_{Sf}(x_1, x_2, x_3, x_4)$.

$$\frac{\partial F_{opt}}{\partial x_1} = \frac{\partial F_{opt}}{\partial x_2} = \frac{\partial F_{opt}}{\partial x_3} = \frac{\partial F_{opt}}{\partial x_4} = 0 \quad (4.52)$$

$$\frac{\partial c_{Sf}}{\partial x_1} = \frac{\partial c_{Sf}}{\partial x_2} = \frac{\partial c_{Sf}}{\partial x_3} = \frac{\partial c_{Sf}}{\partial x_4} = 0 \quad (4.53)$$

Table 4.8 Values obtained for dimensionless variables when calculating F_{opt} and c_{sf} extremes

Scope	x_1	x_2	x_3	x_4	Function value
F_{opt} (3.52)	-1.032	-0.163	-1.317	0.021	$F_{opt\ min}$ = 7.714
c_{Sf} (3.53)	-5.982	-0.42	-1.753	-2.171	$c_{sf\ min}$ = 0.818

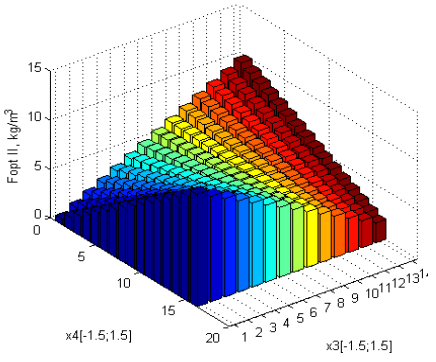

Figure 4.14 Influence of dimensionless factors x_3 and x_4 on the carbon content of the substrate bound in solvents (EBA fermentation, $x_1 = x_2 = 0$)

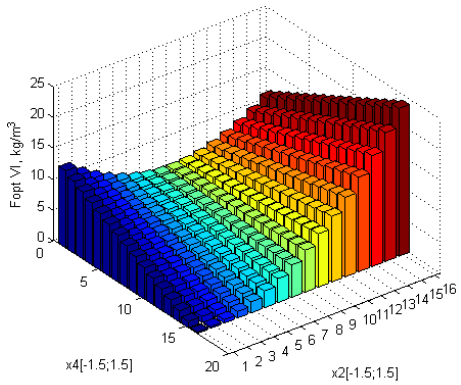

Figure 4.16 Influence of dimensionless factors x_2 and x_4 on the carbon content of the substrate bound in solvents (EBA fermentation, $x_1 = x_3 = 0$)

Selective bibliographic references

[20]. Volesky B., Votruba J., Modeling and Optimization of Fermentation Processes, Elsevier Science, 1992

CHAPTER 5

Biogas by anaerobic fermentation in wastewater treatment plants

This chapter is focused on the problems of biogas production and control of this production in high-capacity industrial installations in Romania.

On average, at a fermentation station, approximately 400–600 m^3 of biogas can be obtained from a tone of waste mixture, of which 50–70% can be methane [2]. As shown before, the entire fermentation process involves four main phases of biomass decomposition:

1. Hydrolysis: Hydrolytic microorganisms convert heavy organic molecules into smaller particles such as sugars, fatty acids, amino acids, water.
2. Acidogenesis: the particles formed in the first phase are decomposed into organic acids, ammonia, hydrogen sulphite and carbon dioxide.
3. Acetogenesis: the formation of hydrogen and carbon dioxide as a result of the transformation of the complex mixture of fatty acids into acetic acid.
4. Methanogenesis: the formation of methane, carbon dioxide and water.

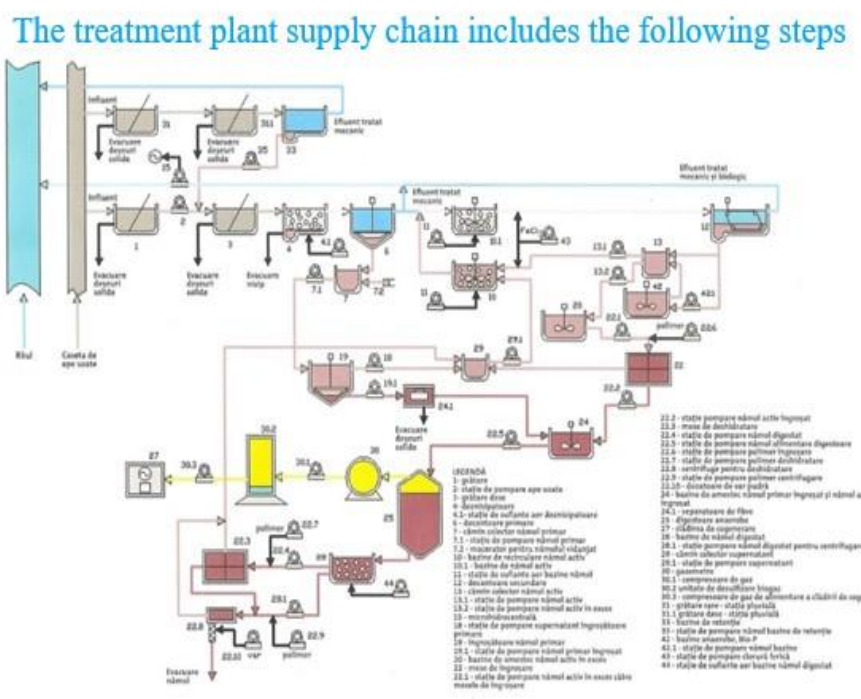

Figure 5.3 - Flowsheet for the technological flow of wastewater purification with active sludge

General data wastewater treatment plant. The purpose of the treatment plant is to purify household, rain and industrial wastewater from urban agglomeration. The treatment

line for these waters is in accordance with the flowsheet in Figure 5.3 includes the following sequences:

- Mechanical treatment by:
    - Dense - rare screens : Dense screens (10 units) with opening between 6 mm bars are intended to retain solid waste from the water to be collected and discharged from the station.
    - Dense screens
- Desnisipation
- Aerobic fermentation
- Primary and secondary decanting: The primary decanters consist of 2 batteries of 4 radial units 55 m in diameter that retain fine and colloidal suspensions by sedimentation. The primary sludge scraped from the base of these decanters is sent to the sludge line for thickening and then to biogas.

The sludge line contains the following steps:

- stabilization of sludge by thickening;

- anaerobic fermentation with biogas production;

- dehydration of stabilized sludge.

Start of the digester. The initiation phase begins with the initial water supply of the digester, which has been heated in an external heat exchanger. Then start feeding with small amounts of raw sludge (primary sludge or excess). During the first 4-5 days it is supplied by about 25 m^3/day, then gradually increase the amount of feed to 50 m^3/day, 80 m^3/day, 100 m^3/day up to 380-480 m^3/day everything over the course of 42 to 45 days. During this period, the first quantities of biogas begin to be obtained from the fermentation process. In the third week (days 14 to 21) gas-producing bacteria are formed. In week four to five (days 28 to 35) the first biogas productions appear. At eight to ten weeks (days 56 to 70) from point 0 (zero) sludge production is reached, the concentration of the active sludge is reached and the normal operating flow rate is reached. The role of gradual feeding at low doses is to facilitate the controlled development of methane-producing bacteria. Throughout the start, the sludge in the digester is recirculated and passed through a heat exchanger outside the digester to ensure and maintain the required temperature of the digester (36°C).

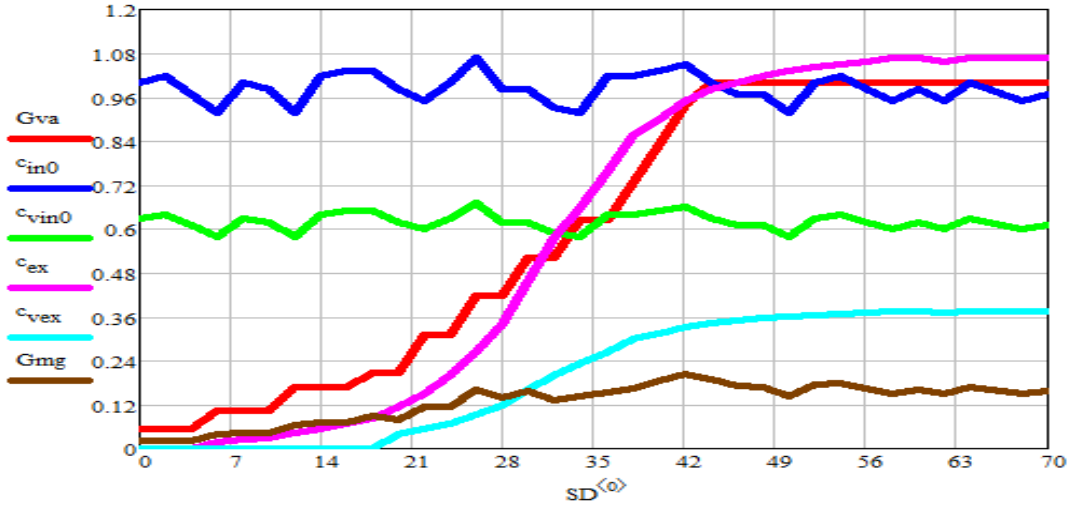

Figure 5.7 Dynamics of starting an active mud digester from wastewater treatment in a large city (Gva= Gvam/480, c_{in0} =c_{inm}/60, c_{vin0}=c_{inm}/60, c_{ex} =c_{exm}/60, c_{vex}=c_{vexm}/60, Gmg=Gmgm/2.88x10^4, concentrations in g/L, flows in kg/day)

Since the bioreactor is full, i.e. it operates without volume variation, its operation during this period can be described mathematically, simplified, as shown by relationships (5.1) - (5.2). A global kinetic for volatiles (c_{ves}) and biomass (c_x) is recognized here.

$$\frac{dc_{ve}}{d\tau} = \alpha \frac{v_{max} c_{ve}}{K_m + c_{ve}} c_x + \beta \frac{v_{max} c_{ve}}{K_m + c_{ve}} + G_{Vg}(c_{vin} - c_{ve}) \quad (5.1)$$

$$\frac{dc_x}{d\tau} = \alpha \frac{v_{max} c_{ve}}{K_m + c_{ve}} c_x + + G_{Vg}(c_{xin} - c_{vex}) \quad (5.2)$$

Biogas from the fermentation process is captured and stored in gas tanks (gasometers). The resulting biogas is analyzed by the gas analyzers to determine its chemical composition.

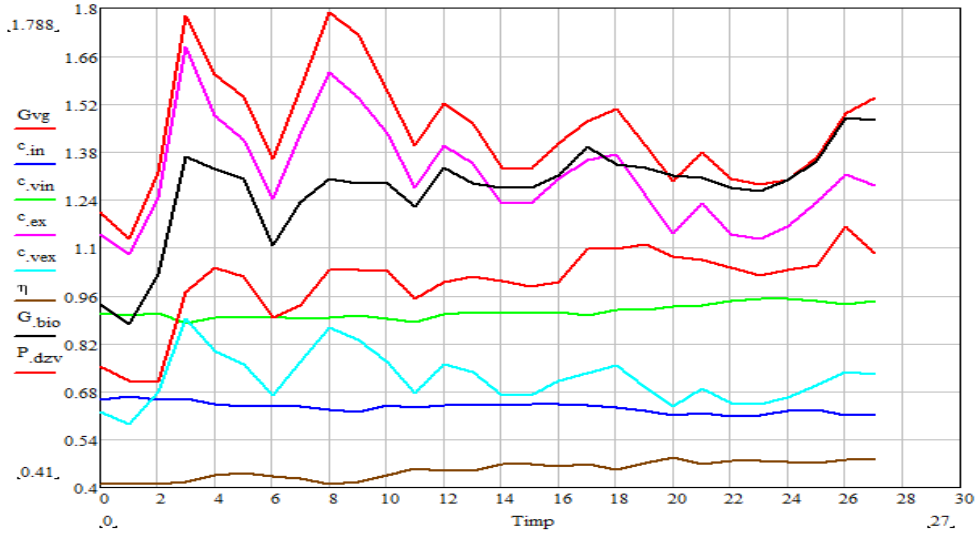

Figure 5.8 Data on the nominal operation of the biogas fermentation station of the active sludge in a plant associated with a large city (Gvg= Gvam/2000, c_{in0} =c_{inm}/60, c_{vin0}=c_{in0}/c_{vin}, c_{ex} =c_{exm}/60,

$c_{vex}=c_{exm}/c_{vexm}$, $G_{bio}=G_{biom}/2.88x10^4$, $P_{dzv}=P_{dzvm}/2000$, concentrations in g/L, flows in kg/day and m^3/day respectively, P_{dzvm} in kW)

This chapter deals with technological aspects of the production of active sludge from the biological treatment of domestic waste water and its use for a biogas plant with cogeneration operation, characteristic to a large city. It has been studied how the bacterial system of methanogenesis occurs when only the addition of inocul is necessary because the fermentation mass already has the bacteria needed for fermentation. The experimental part of this chapter refers to the commissioning of a biogas fermenter (Figure 5.7) and the long-term tracking of the operation of the biogas line coupled with the electric current cogeneration line and hot water for the process (Figure 5.8).

Selective bibliographic references

[2]. Rapport J., Zhang R., Jenkins M. B., Williams B R., Current Anaerobic Digestion Technologies Used for Treatment of Municipal Organic Solid Waste, Biomass and Bioenergy., 35, 3, 1263 -1272, 2011

CHAPTER 6

Conclusions and perspectives

The opening of the paper focuses extensively on the issue of introducing anaerobic fermentation biofuels, namely biobutanol, bioethanol and biogas in the race of present and future energy sources.

Bioethanol is a high-performance biofuel, in addition to its use as engine fuel, it is highlighted in this study the obtaining of bioethanol from corn, for which specific elements are introduced in their own form (scheme of main operations, specific consumptions, considerations on the kinetics of sugarification, considerations on the kinetics of fermentation).

In this case of the production of bioethanol from maize, for better fermentation management that can lead to higher performance than the traditional case, the fermentation control is addressed by coupling with a process of separation of the ethanol produced.

A statistical model is brought as a novelty in the presentation of biobutanol as the biofuel of the future. Under standard fermentation conditions, it shows the dependence of the final concentration of butanol, acetone and ethanol in the product on the process factors, characteristics of the formation and operation of the fermentation medium (substrate concentration (glucose), butyric acid concentration, carbon/nitrogen ratio and fermentation temperature).

The integration of EBA fermentation with gas stripping of solvents, required by their toxicity, on the fermentation clostridia system was carried out according to a new working sequence. This is characterized by the fact that fermentation starts with batch operation then proceeds with fed-batch operation, over which is added the gas stripping. For this complex mode of operation, a mathematical model of 18 differential equations has been developed, in which the kinetic process itself is coupled with the transfer of mass from liquid to the stripping gas of each solvent and water.

The optimization problem was formulated to seek an optimization solution to maximize the fixation of carbon from the substrate into solvents and to minimize the concentration of substrate in the fermentation medium, at the end of the batch, this being developed using statistical modelling as a working tool based on a four-factor orthogonal plan of order 2.

In this paper, it was described how to obtain the reticulated PVA-BC membranes on ceramic support and their characterization by microscopy and FTIR transmission spectra.

For the use of reticulated membranes PVA-BC on ceramic support, in the pervaporation of ethanol-water mixtures, an experimental, easy-to-operate installation was made on a pilot scale in the laboratory. In which the total flow rate of the permeat is measured by measuring the loss of liquid in the liquid chamber of the pervaporation device, while the refractometer measurements determine the concentration of ethanol in the feed and in the condensed pervaporate.

In the experimental investigation of the pervaporation behavior of each membrane type, a two-level experimental plan was used for temperature, permeation pressure in the vapour chamber of the permeation unit and ethanol concentration in the processed mixture.

A consistent analysis was presented for each membrane type on the dependence of permeat flow rate and water separation factor on process factors. Analysis of expressions obtained for pervaporation flow rate and water separation factor for the three membranes used shows that the differences between them are related to the presence of biocellulose in the membrane structure.

A unification procedure was considered in order to add to the permeat flow rate and water separation factor, the fourth factor, represented by the biocellulose content in the membrane. Thus, analytical expressions were formulated for $N_A(x_1, x_2, x_3, x_4)$ and $\alpha_{w/Et}(x_1, x_2, x_3, x_4)$.

In this work, the technological aspects of the production of activated sludge from the biological treatment of domestic waste water and its use for a biogas plant operating with cogeneration, which is characteristic of a large city, have been addressed. The experimental part described the commissioning of a biogas fermenter as well as the long-term tracking of the operation of the biogas line coupled with the cogeneration line of electric current and hot water for the process.

A finding resulting from this analysis is that from 1900 m^3/day sludge supplied in digesters produces 24000 m^3/day of biogas. The cogeneration station powered by two 1000 m^3 gasometers, which operate with two 2 MWh gas engines each, produces electricity and heat.

From the point of view of the research perspective present in this paper, three directions are mentioned: i) for biochemical processes and biotechnology, the search for the most efficient and economical sources of raw materials must continue, closely linked to the deepening of biological pathways of their expression; ii) the development of coupled processes and their analysis through mathematical modelling is a path to a deeper understanding and knowledge of biotechnology with application or potential for industrial application; iii) the role of genetic engineering in the control of microorganisms responsible for bioprocesses, which is now at a promising start, and must continue.